Trends in the Adsorption of Mono-End-Capped Polystyrenes onto Polar Substrates: Theoretical Predictions and Experimental Observations

ZHANG JIAN,[1] RICHARD ZAJAC,[2] AMIT CHAKRABARTI,[2] TANIA DYAKONOV,[1] XIAOYEN GUO,[1] CHRIS SORENSEN,[2] DENNIS BURNS,[1] WILLIAM T. K. STEVENSON[1,3]

[1] Department of Chemistry, McKinley Hall, Wichita State University, Wichita, Kansas 67260-0051

[2] Department of Physics, Cardwell Hall, Kansas State University, Manhatten, Kansas 66506-2601

[3] NIAR, Wichita State University, Wichita, Kansas 67260

Received 12 March 1999; accepted 22 March 1999

ABSTRACT: Predictions of the influence of the solvent quality (χ), the segment–substrate interaction parameter (χps), the chain length (N), and the end cap–substrate interaction parameter (Δ) on the equilibrium-adsorbed amount from a dilute solution of end-functionalized homopolymers (Γ) onto a solid substrate, when both the end cap and polymer segments compete for sites on the surface, were made through application of the self-consistent-field (SCF) theory. These predictions were tested and evaluated through measurement of the equilibrium-adsorbed amount, from a dilute solution of single-end-functionalized custom synthesized relatively monodisperse polystyrenes, possessing an end group (X) chosen to interact with a mildly acidic inorganic substrate (Aerosil 130) and a mildly basic inorganic substrate (aluminum oxide C) through dipole–dipole interactions, hydrogen-bonding interactions, and specific acid–base interactions, as a function of χ, χps, Δ, and N. A protocol was developed for the numerical estimation of Δ through the establishment of dimensionless ratios of the type Γ_X/Γ_H, by experiment and through SCF calculation, as a function of Δ, for polymer/solvent/substrate systems characterized by specific combinations of χ, χps, and N. © 2000 John Wiley & Sons, Inc. J Appl Polym Sci 76: 1422–1447, 2000

Key words: polymer; surface; equilibrium; adsorption; isotherm; SCF

INTRODUCTION

An understanding of interfacial phenomena has been central to many recent successful commercial engineering spin-offs from the fields of polymer science, metallurgy, and ceramics. A broad listing of successes would include the commercialization of fiber-reinforced composites (both organic and ceramic), metal alloys, and polymer blends and new approaches to adhesion technology. An understanding of the solid–liquid or liquid–liquid interface is especially crucial to the efficient stabilization (or destabilization) of suspensions and emulsions in materials and food-delivery systems, the prevention of biofouling on ships hulls and in food-processing plants, and protection against rejection or encouragement of cellular in-growth into medical implants, to name a few. In all these applications, a method of choice for the modification of interfacial properties has

Correspondence to: W. T. K. Stevenson.

Contract grant sponsor: National Science Foundation; contract grant number: OSR-9255223.

Contract grant sponsor: State of Kansas.

Journal of Applied Polymer Science, Vol. 76, 1422–1447 (2000)

been to deposit a very thin layer of organic polymer onto the solid surface from a solution (particulates) or to add a polymer to one of the liquid phases (emulsions) possessing properties which lead to its segregation to the liquid–liquid interface. (We may add that a solution-deposited polymer has been used to modify solid–solid interfaces also, such as in the pretreatment of fibers prior to the preparation of fiber-reinforced composites and in the pretreatment of ceramic precursor powders prior to the sintering process.)

Early investigations of this topic were phenomenologically based and sought to establish relationships among surface chemistry, polymer structure, absorbed amount, and tightness of binding.[1] Over time, theoreticians established analytic and computational tools which were used to establish relationships between those same experimental variables. For example, deGennes established (for homopolymers in a good solvent) that the adsorbed polymer formed a self-similar grid with a dominant length scale equal to the distance from the surface and derived scaling relationships between, for example, the chain length and the segment concentration profile.[2,3] Scaling relationships have been established also for polymer brushes, following the realization that a chain in a brush could be described as a string of statistical units (or "blobs") with a diameter equal to the anchor-to-anchor spacing on the substrate surface.[4] By far the most useful alternative to deGennes' scaling model has been the self-consistent field (SCF) approach.[5,6] Using tools based on these methods, theoreticians (with some resort to experimental verification) have established models which correctly predict the replacement of short homopolymer chains by longer chains of the same structure,[7] the replacement of longer brushes by shorter brushes of the same structure (when replacement is thermodynamically feasible),[8–10] and the replacement of homopolymer chains with others of the same length but with a larger polymer segment–surface interaction energy (χps).[11] The segment density profile of the adsorbed homopolymers and brushes from the surface outward has been calculated,[2,12–14] as has the interacting influence of surface roughness, curvature, and chain length (N) on the absorbed amount (Γ).[15–18] The nature of the surface–segment interaction (and how that interaction can be manipulated)[19–23] and the motional constraints placed upon the adsorbed segment (reversibly or irreversibly adsorbed, able to diffuse across the surface or not, the formation of a "glassy" monolayer, etc.) have all been shown to play a part in determining equilibrium adsorptivity.[24–27]

Theoretical developments have been matched and often inspired by experimental endeavors. For example, the force-balance experiment of Klein and Israelachvili has allowed for the construction of models which shed light upon the nature of the interaction between absorbed layers of a polymer (repulsion, bridging, etc.), which has led to a better understanding of polymer-stabilized colloids and dispersions.[9,10,22,28–32] Multidimensional nuclear magnetic resonance (NMR) spectroscopy has been used to obtain estimates of Γ and the train, loop-tail distribution on the surface, through interpretation of changes in the relaxation spectra as a result of motional constraints imposed on the chain segments and depletion layer thicknesses, when appropriate.[33–35] Attenuated total reflectance (ATR) IR spectroscopy has been used successfully to determine Γ, the proportion of polymer trains on the surface or interface, and the nature of the segment–surface interaction, the kinetics of slow exchange of one polymer for another, insight into preferential adsorption as a function of delta(N), the difference in chain length, delta (χps), the difference in the segment–surface interaction energy, Δ, the interaction energy between an end group and the surface, and global conformational changes with specific reference to adsorbed proteins.[36–54] Ellipsometry has shed light on the effective thickness of the equilibrated layer and on the kinetics of slow-exchange processes,[55–58] as has the newer family of ATM techniques, some of which can be applied *in situ*.[59,60] The calculated chain-segment density profile at the surface is a function of the model used to characterize the adsorption process. For example, deGennes, in an early application of the scaling theory, recovered for strongly stretched brushes a constant segment density from the surface to almost the outer extremity of the brush.[4] In contrast, more recent SFC theory (Milner et al.) points toward a parabolic segment density distribution for the stretched brush.[6] The application of small-angle neutron scattering techniques has allowed for an experimental recovery of the segment density distribution without any prior assumptions.[61–66] In the case of end-grafted chains, a parabolic density profile was recently recovered by neutron scattering for stretched brushes in the absence of interpenetrating chains, thus lending credence to the SCF-based argument.[66]

The initial absorption of a polymer from solution onto a bare surface occurs very quickly, and, until recently, was subject to speculation without a definitive description. However, recent developments in fast response optical reflection spectroscopy[27,67–70] and improvements in the application of FTIR–ATR spectroscopy, ellipsometry, neutron scattering, potentiometric titration, and radiolabeling at short times[71–78] have begun to shed light on the kinetics of this process.

To properly introduce the work described here, we must codify relationships between the experimental variables and the properties of the adsorbed polymer. Therefore, it is necessary to undertake at this point a brief discussion of important theoretical/experimental parameters which influence the adsorption process. For example, the thermodynamic (energetic) interaction between the individual polymer segment and the solvent is usually represented by χ, the Flory–Huggins interaction parameter. Chi (χ) normally varies (in units of kT) from 0.5 for a theta (θ) solvent to 0 for a good solvent which screens out segment–segment attractions. The enthalpy of interaction between an individual polymer segment (ps) and the surface is usually measured as χps (also in units of kT) and is a function not only of polymer structure and surface chemistry, but also of the relative affinities of the polymer segment and solvent for the surface. A solvent which removes polymer from the surface is usually termed a displacer. Segmental adsorption involves a loss of conformational entropy, and so for segmental absorption to occur, χps must exceed some critical value, designated χs—usually a small fraction of kT ($\chi ps > \chi s$). The enthalpy of interaction between a functionalized chain end and the surface is usually measured as Δ kT.

The equilibrium-absorbed amount Γ and the segment volume fraction distribution is a function of the polymer solution concentration. The critical overlap concentration c^* defines a limit below which the solution may be described in terms of the dimensions of the individual coil (Rg, etc.) and above which the solution may be described in terms of a mesh size which is a function of N, χ, and the polymer segment volume fraction in solution, ϕ.[3] If adsorption of a monodisperse polymer onto a surface is performed from a solution below c^*, a standard high-affinity adsorption isotherm with a pseudoplateau is usually produced.[79] If c^* is exceeded, the absorption plateau disappears to be replaced with Γ as a very fast, then monotonically increasing, function of c (or ϕ), while at the same time, the absorbed polymer segment density profile $\phi(z)$ becomes compressed due to screening of the excluded volume interaction by interpenetrating unadsorbed chains.[25,63,71] In both the computational and experimental work described herein, measurements were made below c^* (i.e., $c < c^*$), the former through the choice of modeling conditions ($c^* \sim N^{-0.8}$) and the latter confirmed by recovery throughout of standard, high-affinity experimental adsorption isotherms.

To illustrate this terminology, the global conformation of some isolated adsorbed tethered chains will now be described as a function of key parameters which influence the adsorption process. In all three instances [Fig. 1(a–c)], the end cap–substrate interaction parameter substantially exceeds the critical adsorption parameter ($\Delta \gg \chi s$) and so the chain end (open circle) is attached to the surface. If the solvent is not a displacer for the polymer segment, ($\chi ps > \chi s$), in-chain segments are also adsorbed [Fig. 1(a,b)]. If the solvent quality is poor [$\chi = 0.5$ or higher, (a) in Fig. 1], the adsorbed chain will form into a string of small collapsed Pincus blobs[80] and a pancake configuration will be achieved with a measured high ratio of segments in trains/loops. If χps is fixed as in Figure 1(a), and if solvent quality is improved [$\chi < 0.5$, (b) in Fig. 1], blob size will increase and the proportion of loops increases as segment–segment attractions become screened and unadsorbed segments lift off the surface. If the solvent now becomes a displacer (d) for the polymer segment ($\chi s > \chi ps$), the entire chain is lifted off the surface. The chain dimensions now become similar to the solution radius of gyration (Rg) and become a strong function of χ. Surrounding such a chain with other tethered chains spaced σ units apart on the surface will produce a polymer brush with a characteristic "height" h which scales with N, χ, and σ.[81]

We have undertaken previously to characterize this adsorption phenomenon from a static equilibrium (thermodynamic) and dynamic (kinetic) viewpoint through application of Monte Carlo off-lattice computer simulations via modified Metropolis algorithms. The results of these simulations have been validated through confirmation of recent theory and are mostly consistent with recent experimental observation. In addition, use of this method has given us access to kinetic problems which may not be tackled experimentally, through our ability to, for example, follow the

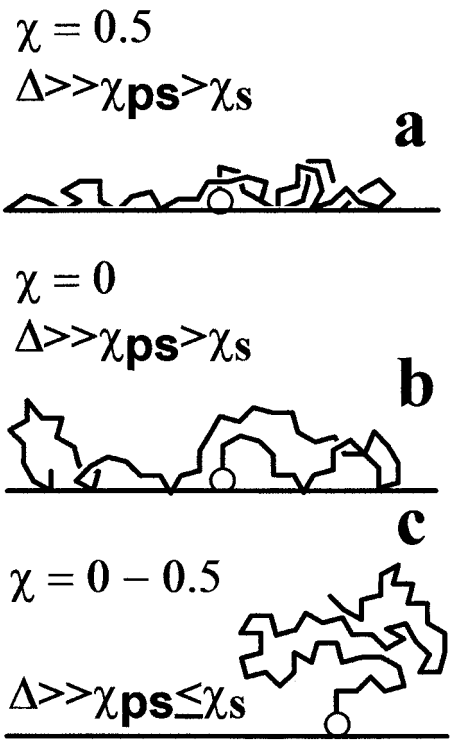

Figure 1 Some possible global geometries of a single-end-anchored chain on a surface: (a) Adsorption from a theta (θ) solvent onto a substrate when in-chain segments are able to displace solvent molecules: Note the flat configuration and high train content; (b) As in (a) but from a good (athermal) solvent: Note the reduced number of trains and increased loop content. (c) Adsorption from a displacing solvent: Coil dimensions are similar to that of the unattached coil in that solvent.

flight of a labeled subpopulation of chains within a larger ensemble of otherwise identical chains.

We have confirmed that the adsorption of end-functionalized polymers from a displacer for the in-chain segments is diffusion-controlled at short times and controlled at longer times by tunneling (reptation) of the chains through an activation energy barrier imposed by other adsorbed chains. The characteristic rinsing time for desorption of these chains in a good solvent was found to exceed the construction time by a wide margin. Shorter displacing chains with the same end-group affinity for the surface were found to be more effective replacers of the original population than were otherwise identical chains with a larger end-group surface interaction (Δ). In both dynamic and equilibrium situations, the dominant length scale was given by the first moment of the density profile, which was parabolic in the absence of, and Gaussian in the presence of, interpenetrating dissolved chains,[82] a finding recently confirmed by an alternative application of SCF and scaling arguments.[83] We also determined that short and long chains in bimodal polymer brushes segregate vertically, in a pronounced fashion in a good solvent and to a lesser extent in a θ solvent.

Segregation in a bimodal brush adsorbed onto a spherical surface was reduced over that observed in a bimodal brush adsorbed onto a flat surface.[84] If adsorption of the end group is *irreversible*, adsorption follows the same path (in this instance, screened diffusion-controlled, then logarithmic, with the formation of an activation energy barrier toward further adsorption). Dissolved chains are completely rejected from the resulting brush which adopts a parabolic density profile with a dominant length scale equal to the first moment of the density profile throughout formation and into the "quasi"-equilibrium regime which develops at late times.[85] On the other hand, the growth of an irreversibly bound layer of a homopolymer was found to proceed in three stages: The vacant site concentration on the surface was filled at an exponentially decreasing rate due to collapse of initially adsorbed coils onto the surface. At the same time, Γ was shown to grow through screened diffusion to the surface. At later times, adsorbed chains are "reeled in" to the surface and Γ increases by reptation of incoming chains through an activation energy barrier. The density profile corresponds to that of a dense layer of trains at the surface followed by an extended brush with a parabolic segment density distribution, much like the density profile adopted by an *A:B* diblock copolymer where one segment is adsorbed strongly and the other not at all.[85]

The labeling capability of the computer-simulation method was used to study the dynamics of adsorption of reversibly bound homopolymers. *Most importantly, we recovered the self-similar mesh predicted by deGennes for homopolymers adsorbed at the critical overlap concentration*. Chains adsorbed early expressed a high proportion of trains while those adsorbed at later times were more loosely bound. Although an equilibrium distribution of trains, loops, and tails was established for the overall population, individual chains were shown to move to and from this equilibrium distribution very slowly as they adsorbed to and desorbed from the surface in a process governed by exponential kinetics. The existence of a loosely bound subpopulation of chains which "flutters" on and off the surface was established.

Incoming chains with identical N, but with higher χps, were found to be more efficient displacers than were longer incoming chains with identical χps. When $d(\chi)ps$ is large, detachment of the leaving chain appears to be assisted kinetically by the presence of adjacent segments of the incoming polymer.[86]

In this communication, we attempted to integrate experiment and theory and explore the scope and limitations of computer-assisted SCF analysis in predicting experimentally observable trends in the absorption of single-end-capped polymers from a dilute solution onto a solid substrate, under conditions where both the end cap and in-chain segments compete for sites at the surface. To this end, we have custom-synthesized a series of polystyrene polymers possessing differing end-cap functionality and measured the equilibrium adsorption (Γ) of those polymers from a good and a θ solvent onto previously characterized inorganic substrates, chosen to interact with the end cap in a specific well-understood fashion. Experimentally observed trends in Γ, as a function of N, χ, χps, and Δ, were measured and compared with predictions from SCF. We finish by outlining conditions under which SCF can be combined with experiment to estimate Δ, the end cap/substrate interaction parameter, for a single-end-functionalized polymer under these conditions.

EXPERIMENTAL

Polymer Synthesis

General Comments

Polymers were synthesized in glassware on a high-vacuum manifold using a rotary and diffusion pump with liquid nitrogen cold traps. Reagents (AR, HPLC grade, or the purest available) were purchased from Aldrich (Milwaukee, WI), Polysciences (Warrington, PA), or Fisher Scientific (Pittsburgh, PA). Early reagent purifications were performed, under O_2-free and dry nitrogen which had been purified by passage through an activated copper catalyst and molecular sieve, in Schlenkware or in a glove box. Glassware was soaked in chromic acid, a strong base, and then distilled water and dried before use.

Solvents

THF and benzene/cyclohexane (B/CH) mixtures were stored over molecular sieves, then refluxed under nitrogen over sodium metal (Na)/benzophenone (BP) until blue/black (THF) or pale green (B/CH), then distilled into a volume-calibrated vacuum flask over Na/BP, degassed and stored on the vacuum line until flash distillation into the polymerization reactor.

Monomer

Styrene (S) was distilled with cuts under reduced pressure into a volume-calibrated vacuum flask/burette containing freshly ground CaH_2 and a home-made glass-covered magnetic stir bar. The monomer was stirred 1–2 days in a bulb attached to the burette, degassed, then flash-distilled with cuts from the burette into the polymerization reactor.

Initiators for Polymerization

Initiators for polymerization were handled in clean gas-tight Hamilton syringes. sec-Butyl lithium (sBLi, Aldrich) was standardized using the Gillman double-titration,[87] revealing good batch-to-batch conformity ($\sim$1.3M sBLi, $\sim$0.55M basic impurity). 3-Dimethylaminopropyl lithium (DMAP–Li) was prepared using a variant on published recipes.[88,89] *Example*: Eight and one-half grams 3-dimethylaminopropyl lithium chloride (DMAP–Cl) was obtained from about 17 g 3-dimethylaminopropyl chloride hydrochloride (DMAP–HCl) by reaction with a double molar amount of 50% NaOH (aq). DMAP–Cl was decanted off, filtered, dried over KOH pellets at -20°C overnight, decanted into a vacuum flask, and degassed. Clean lithium shot (-4 to $+16$ mesh, 1.2 g) was added to a Strauss flask with a glass stir bar. THF ($\sim$30 mL) and DMAP–Cl (8.0 g) was flash-distilled into the Straus flask. The mixture was stirred at ~ -30°C for 8 h, standardized using the Gillman method, and stored at -70°C for 3 days max before discarding. (Example: Approximately 0.4M DMAP–Li, $\sim$1.0M basic impurity).

Carbon Dioxide

Carbon dioxide (CO_2: quantified using the ideal gas law with n = PV/RT, etc.) was bled through a Drierite $CaSO_4$ drying cartridge and a vacuum line with a mercury manometer into a vacuum flask containing an activated 4Å molecular sieve and condensed into the sieve at -70°C. The flask was pumped on to remove residual air and some CO_2, then warmed to room temperature, and the

evaporated CO_2 was condensed into a second large volume-calibrated vacuum flask with a cold finger (leaving behind any residual water in the molecular sieve), degassed, and stored until use.

Polymer Characterization

Intrinsic Viscosity

Dilute solution viscosities were recorded in toluene at 30 ± 0.05°C using a modified Ubbelohde viscometer[90] with a solvent drop time of 166 s. Polymer intrinsic viscosities [η, mL/g] were obtained as $(\eta sp/C)_{C\to 0}$ and $(\ln \eta r/C)_{C\to 0}$ from Huggins[91] and Kraemer[92] plots of the data.

Thin-layer Chromatography (TLC)

TLC separations were carried out using established procedures for small molecules,[93] but with additional care to produce small and symmetric spots which undergo less "smearing" on development. (A polymer was dissolved to a fixed concentration and spotted using a 1 μL GC syringe.) Separations were performed on dry silica and neutral alumina plates (Alltech) with a UV-254 fluorescent indicator.

Size-exclusion Chromatography

SEC was performed using a Shimadzu LC-8A HPLC pump, a Jordi-Gel mixed-bed precolumn (50 × 10-mm i.d.), a Jordi-Gel mixed-bed SEC column (500 × 1-mm i.d.), a Shimadzu RID-6A refractive index detector, and Polymer Laboratories data collection hardware and data manipulation software, running on a Gateway P5-60 PC.

IR Spectroscopy

Polymers were examined as thin films cast onto NaCl salt plates using a Mattson research-grade FTIR spectrometer with an MCT detector.

NMR Spectroscopy

Proton and carbon-13 spectra were obtained in $CDCl_3$ with TMS as the internal reference using a Varian XL-300 NMR spectrometer.

Polymer Derivatization

General Comments

Carboxylate-terminated polymers (PS–COOH) were derivatized using variants on established procedures, made necessary by problems related to polymer solubility and recovery after reaction.

Reduction to Alcohol

Example: PS–COOH (0.5 g) was dissolved into THF (20 mL) under N_2 and stirred ~3 h at room temperature with $NaBH_4$ (0.05 g), then stirred ~6 h with I_2 (0.05 g). HCl (3 mL, 3*N*) was carefully added and the mixture filtered. The polymer was precipitated in methanol (×2) and vacuum-dried.[94]

Esterification to the Methyl Ester

Example: PS–COOH (0.5 g) was dissolved in benzene (40 mL) and methanol (12 mL) under N_2 and stirred ~3 h at room temperature with trimethylsilyl diazomethane (Aldrich, 1 mL, 2.0*M* in hexane). The polymer was precipitated in methanol (×2) and vacuum-dried.[95]

Adsorption Experiments

Aerosil 130 and ALOC Substrates

Aerosil 130 [Degussa AG (Frankfurt, FDG), pyrogenic silica, CAS-Reg. #112945-52-5 (ref. 96)] and ALOC [Degussa AG, basic aluminum oxide C (ref. 97)] were activated at 200–250°C for ~3 h under a hard vacuum before use. BET surface areas were measured after activation.[98] The dried substrate was weighed and handled under a N_2 blanket.

Solvents and Solutions

Carbon tetrachloride (CCl_4, AR grade) was double-distilled from a molecular sieve just before use. UV spectroscopic-grade cyclohexane (CH) was refluxed over sodium metal and distilled just before use. Solvent-free polymer was weighed and dissolved into solvent in a volumetric flask and made up to the volume marker at 35°C. Solvents and solutions were handled under a N_2 blanket using clean gas-tight syringes.

Adsorption Experiment

The polymer solution and adsorbent were mixed in hand-made glass flasks (sketched in Fig. 2, top right). The flask was partly filled with the substrate and polymer solution, sealed, and placed on its long axis in a Precision #25 shaker water bath so that the shaker produced a continuous "wave" motion in the polymer solution which broke onto

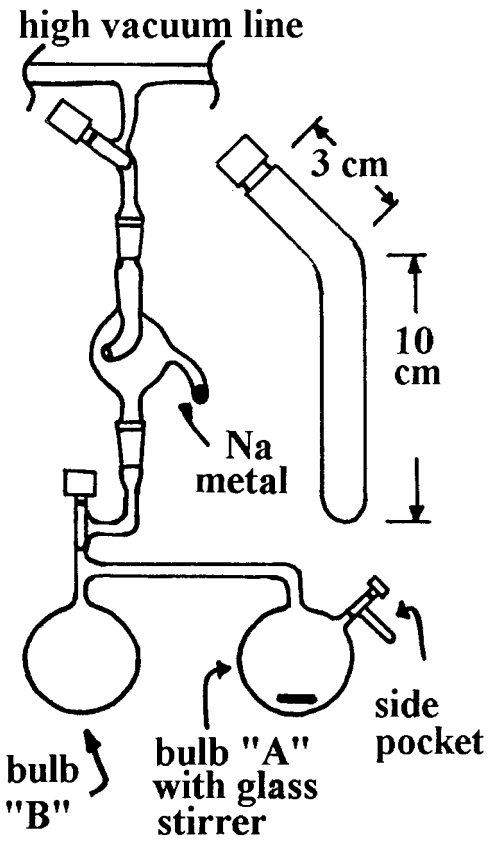

Figure 2 Hand-made glassware used in polymer synthesis and in adsorption experiments. Bottom: Two-bulb reactor with isolable side pocket, attached to vacuum line through bulb with sodium mirror. Top right: Bent ampule used in polymer-adsorption experiments.

the ends of the container. Aluminum foil under an elastomeric cap gasket ensured a perfect seal during the 24–48-h experiment. *Example*: A polystyrene solution (10 mL, 3 mg/mL) was mixed with an adsorbent (0.05 g) and shaken (35°C, 24 h) in three flasks to reach adsorption equilibrium. The vessels were then removed from the shaker and placed vertically in a water bath at 35°C for at least 4 h. The adsorbent was allowed to compact to the bottom, the plastic lid was removed, and the supernatant was withdrawn through a small hole made in the aluminum gasket with a 20-mL syringe equipped with a 22 G 1.5-in.-long needle, threaded into small bore polyethylene tubing for transferring solution from the shaking tube to the syringe. The supernatant was transferred to a 0.1- or 1.0-cm path length Spectrasil quartz cell (depending on the solvent and polymer concentration) through a 0.1-μm Teflon syringe filter and assayed directly by UV spectroscopy in a thermostated cell holder at 35°C.

UV Spectroscopy and Measurement of C(Equilibrium)

All UV measurements were carried out at 35°C using an HP 89532 K UV-visible diode array spectrometer. Residual equilibrium polymer concentrations were read from UV absorption calibration curves of polystyrene [C (mg/mL) versus A (au)] in carbon tetrachloride and in cyclohexane at 262 nm for both the 1.0- and 0.1-cm cells used by us. An average from the three experiments yielded C(equilibrium, mg/ mL) for one point on a Γ(equilibrium, mg/m^2) versus C(equilibrium, mg/mL) curve, with an relative error less than 5% of the magnitude of C.

UV Spectroscopy and Measurement of the Adsorbed Amount, Γ(Equilibrium)

The adsorbed amount, Γ(equilibrium, mg/m^2) corresponding to C(equilibrium, mg/mL), was calculated by application of one of the two equations outlined below:

$$\Gamma(\mathrm{SiO_2}) = \frac{(Ci - C\mathrm{eq})XV}{SA(110)XW}$$

$$\Gamma(\mathrm{ALOC}) = \frac{(Ci - C\mathrm{eq})XV}{SA(88)XW}$$

where Ci is the initial concentration of the polymer in a solution (mg/mL); Ceq, the equilibrium concentration of the polymer in solution (mg/mL); V, the volume of polymer solution (mL); W, the weight of the adsorbent (g); SA, the specific measured surface area (m^2/g); and Γ, the adsorbed amount (mg/m^2).

Measurement of Γ(Plateau)

Data pairs [x = C(equilibrium), y = Γ(equilibrium)] were placed on a scatter plot and Γ(plateau, mg/m^2) was estimated as the average of Γ(equilibrium) data points on the horizontal portion of the curve. Relative errors were less than 10% of the measurement itself.

SCF Calculations

The SCF calculations performed in this study are straightforward applications of the method outlined by Scheutjens and Fleer.[99] Here, the system

is discretized into layers which lie parallel to the adsorbing surface, along a cubic lattice with unit dimension "a." For most calculations, the polymer chains have been taken to contain 200 segments of length a. (We found previously that a chain length corresponding to 100 segments is sufficient to capture the behavior of long chains.)

To each layer i, we associate a probability $p(i)$, which represents the probability of successfully placing a monomer in that layer. Here, $p(i)$ is normalized with respect to its value in the bulk, where there is a bulk monomer density, ϕ_0, which is chosen as a parameter. These probabilities depend on the local concentration of monomers, $\phi(i)$, which we initially represent with some convenient "best-guess" distribution. They further depend on the enthalpy of adsorption for monomers at the surface and the solvent quality, which enters here in terms of the Flory–Huggins parameter χ.

From these probabilities, we construct the configurational probabilities for all possible paths of the chains along the lattice. By averaging over these weighted chain configurations, one obtains a new result for $\phi(i)$. This new result is then used to generate new layer probabilities, leading to a new $\phi(i)$. This process is continued until successive results for $\phi(i)$ differ by less than 10^{-8} monomers/cubic angstrom. Here, multichain effects are implicitly accounted for by virtue of the fact that each chain conformation interacts with the local concentration of the monomers *from all possible configurations*. It has been verified that the use of different initial "guesses" for $\phi(i)$ leads to convergence to the same solution. When convergence is achieved, the adsorption is calculated by integrating $\phi(i)$ while discarding contributions from chain configurations which do not touch the adsorbing surface (so-called nonadsorbed chains).

Now, the difference between a good solvent and a solvent at the theta (θ) point occurs in the expression for the layer probabilities $p(i)$:

$$\ln[p(i)] = \chi a^3(<\phi(i)> - <\phi^0(i)>) + \ln[a^3\phi^0(i)] \quad (1)$$

where $\phi^0(i)$ is the local concentration of solvent molecules and the angular brackets denote averaging over nearest neighbors. Also, χ is the dimensionless Flory–Huggins parameter which is related to the monomer–solvent, solvent–solvent, and monomer–monomer interaction energies[3] by

$$\chi = \chi_{MS} - 1/2[\chi_{SS} + \chi_{MM}] \quad (2)$$

The first term in eq. (1) arises from differentiating the energy of mixing, U_{mix}/kt, where

$$U_{mix}/kt = a^6\chi\Sigma_i<\phi^0(i)><\phi(i)> \quad (3)$$

with respect to the number of monomers in the layer, under conditions of constant volume (i.e., taking out a solvent molecule for every monomer that we add). The second term corresponds to the entropy associated with the solvent molecules and is essentially analogous to the excluded volume effect. It has the effect of making the probability of placing a monomer in the layer to be proportional to the unoccupied volume fraction of the layer, $[1 - a^3\phi(i)]$.

Now, away from the surface, monomers in a good solvent would be no different from the solvent molecules. Thus, we would take $\chi_{MM} = \chi_{SS} = \chi_{MS}$, and so $\chi = 0$. This is the case where monomers interact via the excluded volume only. However, in a theta (θ) solvent, there is no net interaction between monomers, so $\chi_{MM} = 0$, leading to $\chi = 0.5$. In this way, the solvent quality is controlled by selecting an appropriate value of χ for the calculation. A more thorough derivation of these probabilities is presented in the original reference.

Applying this formalism, we note that $\Gamma = \Sigma_{(\text{layers } i)}\,\phi(i)_{ads}$, where $\phi(i)_{ads} = \phi(i)_{total} - \phi(i)_{free}$, and $\phi(i)_{total}$ is the volume fraction of the monomers in layer I; $\phi(i)_{ads}$, the volume fraction of adsorbed monomers in layer I; and $\phi(i)_{free}$, the volume fraction of unadsorbed monomers in layer i.

By this method, we enumerate Γ in terms of equivalent monolayers. (For example, if $\Gamma = 2.1$, sufficient polymer has been adsorbed to ensure that if the adsorbed chains were rendered, and if all the repeat units were close packed on the surface lattice, we would establish 2.1 monolayers of coverage on the surface.)

RESULTS AND DISCUSSION

Polymer Synthesis, Characterization, and Derivatization

Polymers were synthesized to establish experimental trends in polymer adsorption (Γ) versus

molecular weight, χ, χps, and Δ, under conditions where a single functionalized end competes with in-chain segments for surface sites. Our goals were best met using a polymer with $\chi ps \leq \sim 2$. To simplify data interpretation,[7,100] we used monodisperse polymers. To this end, we chose to prepare polymers from the styrene monomer, which have been shown to yield χps values in this range, upon adsorption from common organic solvents onto common inorganic substrates.[40,41,43,44,101–103] Fortuitously, polystyrenes may be prepared by anionic polymerization of styrene,[104] which affords both a convenient route to a monodisperse polymer and a useful aid in end-group functionalization. In all instances, reagent levels were adjusted to yield a target number-average degree of polymerization (Xn) determined by the well-known relationship

$$Xn = \text{\# moles monomer/\# moles initiator}$$

Polymers were synthesized with a weakly acidic carboxylic acid single-end cap and with a weakly basic dimethylamino single end cap, both of which are able to bind to surfaces via specific acid–base interactions, yielding high values for Δ. The former, we termed "Series A" polymers, and the latter, "Series D" polymers. We also prepared polymers end-capped with a polarizable methyl ester functionality ("C"-type polymers) and polymers end-capped with polar and hydrogen-bonding hydroxyl functionality ("B"-type polymers). Nonfunctionalized monodisperse "PS–H"-type polymers were purchased from Polysciences.

The choice of the polymerization initiator and terminator was determined by the nature of the desired end-cap functionality. For example, a single-end carboxylic acid end-capped (Series A-type) polymer was initiated using sBLi and-terminated by reaction with carbon dioxide, then methanol (a proton donor), as summarized in Figure 3(I). In contrast, single-end dimethylamino end-capped (Series D polymer was initiated using DMAP–Li and terminated with methanol [Fig. 3(IV)]. Polymerizations were performed in a two-bulb reactor (Fig. 2, bottom). The entire assembly was evacuated and a lump of sodium metal was carefully heated and evaporated into a modified splash trap containing a small amount of quartz wool to create a reactive sodium mirror through which reagents were distilled for final purification. Polymerization conditions thereafter were determined by the nature of the initiation and

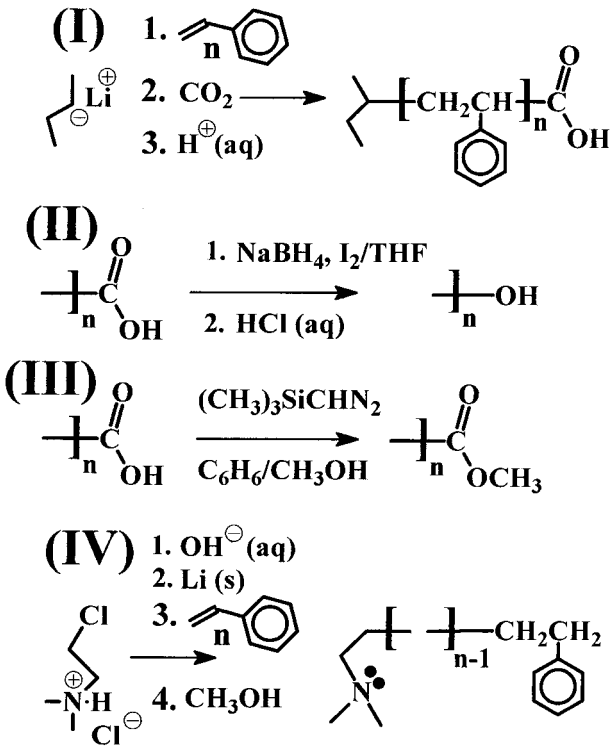

Figure 3 Synthetic pathways: (I) Preparation of carboxylic acid-terminated polystyrene. (II) Conversion of the end carboxylate to an alcohol. (III) Conversion to the methyl ester. (IV) Preparation of dimethylamino-terminated polystyrene.

termination reactions and differed considerably for Series A- and D-type polymers.

Carboxylic acid-terminated (Series A) polymers were prepared by initiation with sBLi and termination with carbon dioxide [Fig. 3(I)]. To minimize side reactions (coupling, etc.), carboxylations were performed in THF solvent.[105,106] Unfortunately, alkyl lithiums are unstable in THF at room temperature,[107] and so these polymerizations had to be performed at -75°C. A fast initiation reaction is preferred, as it will lead to a narrow chain-length distribution ($Xw/Xn \approx 1 + 1/Xn$).[108,109] However, in practice, almost instantaneous initiation and polymerization, such as is obtained with sBLi in THF at -75°C, will produce a broad distribution, as the reaction outpaces the mixing process. We, therefore, had to mix the initiator and solvent, then add the monomer slowly with good mixing to ensure that all chains grew at a similar rate. With reference to Figure 2 (bottom), the sBLi solution was first sealed into the side pocket of the reactor under nitrogen. The flask was attached to the vacuum line and evac-

uated, and the sodium mirror was formed. The THF solvent (~120 mL) and purified styrene (example: ~10 mL) were then distilled into bulb B and warmed to room temperature. The flask was sealed and removed from the vacuum line, and the initiator was transferred to bulb A. Bulb B was cooled to 0°C, bulb A was cooled to −75°C, and the volatile solvent and the less volatile monomer were carefully distilled into bulb A with stirring. The appearance and persistence of a pale yellow color accompanied a successful reaction. About 1 h after distillation was complete, the contents of bulb A were frozen in liquid nitrogen and carbon dioxide was condensed into the flask. The liquid was thawed, and the yellow color disappeared as the chain ends reacted with carbon dioxide. The reactor was opened and about 1 mL methanol was added to ensure protonation of the chain ends. The polymer was recovered by precipitation into excess methanol containing a few drops of 0.1*N* HCl and vacuum-dried to a constant weight.

Dimethylamino-terminated (Series D) polymers were prepared by initiation with DMAP–Li, then by termination with methanol (Fig. 3[IV]). Polymerizations were performed at room temperature in a mixed cyclohexane/benzene solvent to ensure a fast initiation and a moderate reaction rate in a solvent mixture which would not crack the reaction flask in freeze/thaw cycles. With reference to Figure 2 (bottom), the cold initiator was first added to the side pocket under nitrogen. Excess cold initiator (~1 mL) was also added to bulb A to clean the glass reactor and solvent mixture. The initiator solvent (THF) was quickly distilled off from both the side pocket and bulb A to prevent reaction with the initiator at room temperature. The side pocket was sealed, and benzene/cyclohexane (50/50 by volume, ~100 mL) was distilled through a sodium mirror into bulb A. After shaking to dissolve the initiator, the liquid was decanted into bulb B and then distilled back to bulb A. The process was repeated (×2) to separate out the clean solvent in bulb A and the excess involatile initiator residue in bulb B. The conditioned solvent mixture was used to wash the initiator from the side pocket into bulb A. Bulb A was then frozen at −196°C and styrene was distilled into A. The polymerization was carried out in A at 30–35°C for about 6 h, after which the pale yellow color was removed by termination with methanol. The reaction mixture was removed from A, taking care to avoid contact with the initiator residue in B. The polymer was recovered by precipitation into excess methanol containing a few drops of 0.1*N* KOH and vacuum-dried to a constant weight.

Carboxylic acid end-cap functionality in low and high molecular weight Series A polymers were derivatized to the corresponding alcohol and ester derivatives using simple one-pot reactions. Acid functionality was converted to the corresponding alcohol by reaction with $NaBH_4$ and I_2 [Fig. 3(II)][94] and to the corresponding ester by reaction with trimethylsilyl diazomethane [Fig. 3(III)].[95] Reaction conditions were modified to retain polymer solubility throughout, and workups were modified to allow for purification of the involatile polymer. By these means, we were able to generate carboxylic acid, ester, and alcohol, single-end-terminated polystyrenes with essentially the same molecular weight.

Prior to molecular weight determination and adsorption experiments, polymers (A, B, C, and D) underwent purity checks for residual solvent content and adventitious oxidation by FTIR and proton and ^{13}C-NMR spectroscopy. Polymers were ground to a powder, vacuum-pumped in a warm oven, then examined by NMR spectroscopy for residual solvent. The process was repeated until solvent signals merged with baseline noise in the NMR spectrum of a concentrated polymer solution. The FTIR spectra of solvent-free end-capped polymers were compared by interactive subtraction with the FTIR spectrum of pure polystyrene (Polysciences). Aside from small discrepancies which could be attributed to the end cap in low molecular weight polymers at ~3400 cm^{-1} (OH, COOH), ~1700 cm^{-1} (COOH), and ~1740 cm^{-1} ($COOCH_3$), spectra could be completely subtracted, suggesting a high degree of purity throughout.

Polymers were examined by TLC to allow for a qualitative ordering of the sticking probability (or Δ) for end-cap functionality[110,111] and to yield some estimate for the efficiency of functionalization. TLC retention factors (*Rf*) for polystyrenes have been shown to scale as a measurable function of chain length from nondisplacing solvents,[112] and, so, for a proper comparison emphasizing chain-end effects, polymers were required to possess similar and low molecular weights and to be developed using a solvent (e.g., benzene) which displaces styrene segments from the surface.[103] A visual comparison is made in Figure 4 of the *Rf* values for polymers with similar (short) chain lengths and with differing end caps, adsorbing from benzene onto activated silica (top) and

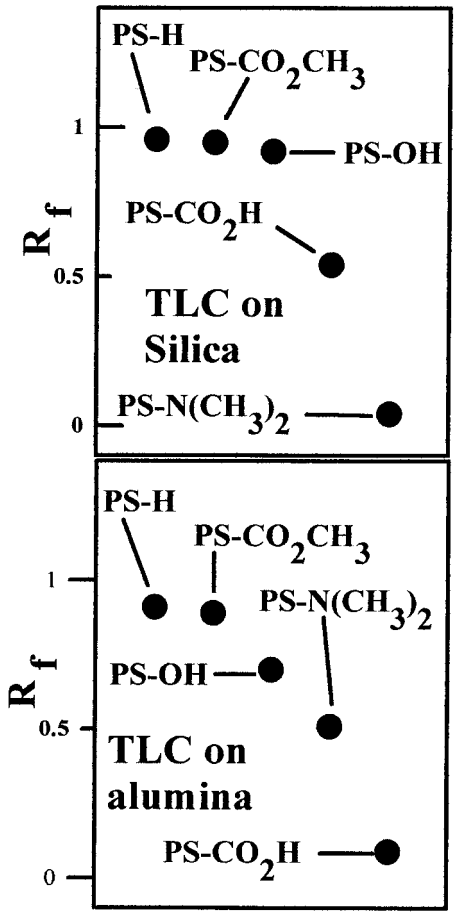

Figure 4 TLC of polystyrenes with similar chain lengths but with differing end groups, from benzene onto (top) silica and (bottom) alumina. X = —CO_2CH_3, —OH, and —COOH corresponds to M = 10 kD; X = —H corresponds to M = 6.9 kD; X = —$N(CH_3)_2$ corresponds to M = 23 kD.

onto neutral (or partly neutralized) alumina (bottom). As expected, nonfunctionalized polystyrene (PS–H) expressed an enhanced mobility over end-capped polymer on both surfaces. Chi_{ps} (χps) for the styrene segment adsorbing from a nondisplacing good solvent (CCl_4) onto silica has been estimated as ~1 kT.[41] In contrast, χps for the methyl methacrylate (methyl ester-containing) segment onto silica from CCl_4 has been estimated as ~4 kT,[41] and, so, the slight reduction in the measured mobility of the methyl ester-terminated polymer ($\Delta \sim 4$ kT from CCl_4) over silica was unremarkable.

A similar reduced mobility of the ester end-capped polymer compared with nonfunctionalized polystyrene onto alumina suggests a similar ordering of sticking enthalpies onto that surface. As expected, the more polar hydroxyl end cap further decreased the mobility of polystyrene over both silica and alumina. The reversed relative mobilities of carboxylic acid and dimethylamino-terminated polymer in benzene over silica and over alumina are a reflection of specific acid–base interactions between the end cap and the surface. For example, silica surfaces are slightly acidic (pK_a ~9.5)[112] due to partial ionization of silanols on the surface and, so, the weak equilibrium

$$\sim Si—OH + \sim NR_2 \rightleftharpoons \sim Si—O^- + \sim NHR_2^+$$

may be envisaged as contributing to the near immobilization of dimethylamino-terminated polymer over silica. In contrast, alumina surfaces are intrinsically basic, due to surface aluminum oxides or hydroxides (if wet).[113] We may envisage even over "neutral" alumina the reactions

$$\sim COOH + O^{-2} \rightarrow \sim COO^- + OH^-$$

$$\sim COOH + OH^- \rightarrow \sim COO^- + H_2O$$

as contributing to the near immobilization of carboxylic acid-terminated polystyrene over alumina. ($\Delta - \chi ps$) for a single COOH functional group on a polystyrene chain adsorbing from CCl_4 onto silica has been measured as ~6.4 kT.[39] If χps for polystyrene under these conditions is ~1 kT,[41] then Δ (~COOH) is ~7.4 kT. From examination of the sketches in Figure 4, it would be reasonable to suggest that the Δ values for the dimethylammonium ion ($\sim NHR_2^+$) from CCl_4 onto silica and for the carboxylate group ($\sim COO^-$) from CCl_4 onto basic alumina are considerably greater than 7.4 kT ($\Delta \gg 7.4$ kT).

TLC was also used as a sensitive qualitative tool for the evaluation of the end-capping efficiency during polymer synthesis and derivatization. For example, partially COOH end-capped polystyrene would separate into two well-separated spots from benzene onto silica. (PS–H and PS–COOH). After partial derivatization to the alcohol, the partly carboxylated polymer would separate into three spots (PS–H, PS–COOH, PS–OH). We were unable to detect impurity fractions in either the as-synthesized (A and D) or derivatized (B and C) polymers after development of overloaded TLC plates, and so we may assume quantitative functionalization of those polymers.

Table I Polymer Molecular Weights

Polymer No.	End Group	M_v[a] ($\times 10^{-3}$)	M_n[b] ($\times 10^{-3}$)	M_w[c] ($\times 10^{-3}$)	M_w/M_n[d]	M_p[e] ($\times 10^{-3}$)
A1	—COOH[f]	10	5.76	9.07	1.57	5.87
A2	—COOH[f]	20	12.1	16.2	1.34	12.6
A3	—COOH[f]	40	25.2	30.6	1.21	23.6
A4	—COOH[f]	97	81.4	90.4	1.11	86.5
A5	—COOH[f]	300	279.5	351.0	1.26	289.4
B1 (from A1)	—OH[g]	10	6.18	11.5	1.86	6.00
B5 (from A5)	—OH[g]	300	295.7	355.2	1.20	289.4
C1 (from A1)	—$COOCH_3$[h]	10	5.91	13.7	2.32	5.82
C5 (from A5)	—$COOCH_3$[h]	300	294.3	352.8	1.20	291.8
D1	—$N(CH_3)_2$[i]	23	15.8	17.6	1.11	18.8
D2	—$N(CH_3)_2$[i]	31	20.4	23.1	1.13	25.0
D3	—$N(CH_3)_2$[i]	63	31.1	47.9	1.54[j]	56.0
D4	—$N(CH_3)_2$[i]	150	113.3	141.5	1.25	156.2
D5	—$N(CH_3)_2$[i]	390	359.9	415.9	1.16	438.9
PS-7[k]	None	6.93	6.86	7.08	1.03	6.99
PS-50[k]	None	45.7	45.6	50.0	1.10	48.9
PS-200[k]	None	?	190.5	200.0	1.05	200.9
PS-400[k]	None	401.3	392.0	400.0	1.02	402.1

[a] M_v: viscosity-average molecular weight from the intrinsic viscosity in toluene at 30°C.
[b] M_n: number-average molecular weight by SEC in dioxane.
[c] M_w: weight-average molecular weight by SEC in dioxane.
[d] H_w/M_n: heterogeneity index (HI) as a measure of polydispersity.
[e] Mass corresponding to detector maximum by SEC in dioxane.
[f] —COOH: carboxylic acid end cap.
[g] —OH: hydroxyl end cap.
[h] —$COOCH_3$: methyl ester end cap.
[i] —$N(CH_3)_2$: dimethylamino end cap.
[j] Bimodal distribution with small overlapping low mass peak. HI includes both peaks.
[k] Purchased from the Polysciences and characterized by them.

Polymer intrinsic viscosities [η] were determined by application of dilute solution viscometry.[90–92] Viscometric molecular weights (M_v), derived from the intrinsic viscosities [η] in toluene at 30 ± 0.05°C using the M–H–S relationship ([η] = K M_v^a),[114,115] with $K = 11.0 \times 10^{-3}$ and $a = 0.725$,[116] are reproduced in Table I, column 3. Plots of the reduced specific viscosity versus the concentration were linear throughout and gave no indication of any concentration-dependent end-group association in toluene as a dilute solution. Number-average (M_n) and weight-average (M_w) molecular weights were determined by SEC[117] and are listed in Table I, columns 4 and 5, respectively, along with heterogeneity indices (HI, M_w/M_n, column 6), given as a measure of the polydispersity. Both Series A and D polymers were shown to encompass a wide range (~1–2 decades) of chain lengths from under 10 kD to over 200 kD. HI were only moderately low (>1.1 throughout). Molecular weight distributions were relatively symmetrical, as evidenced by comparison of M_n and M_p (column 7) values. Derivatization of the chain ends (A1 → B1 and C1, A5 → B5 and C5) did not appreciably change the molecular weight but did broaden the HI of the lower molecular weight polymer.

Polymer Adsorption Experiments

Substrates for polymer adsorption were chosen in order to interact with the adsorbing polymers in specific ways. The requirement that adsorption from organic solvents be onto a surface rather than into a solvent-swollen interphase was met through use of inorganic substrates. The two major series of polymers prepared for these studies (Series A, weakly acidic, and D, weakly basic) are able to form strong secondary acid–base-type complexes, and so we chose substrates with complimentary surface chemistry (as discussed previously with reference to the TLC experiments) to maximize end-cap adsorption enthalpies. Aerosil 130™ (Degussa AG) was chosen as a model mildly

Table II Substrates for Adsorption Studies

Product	Aerosil 130™	Aluminum Oxide C (ALOC™)
Supplier	Degussa AG, Germany	Degussa AG, Germany
Description	High surface area colloidal silica with uniform particle size $\sim \mu$ and shape[a]	High surface area colloidal alumina with uniform particle size $\sim \mu$ and shape[a]
Activation	200–250°C for 3 h under vacuum	200–250°C for 3 h under vacuum
BET surface area after activation	110 m^2/g[b]	88 m^2/g[b]
Internal pore structure	Negligible[a]	Negligible[a]
Surface functionality	Si—O—Si and Si—O—H	Al^{3+}, O^{2-}, and OH^-
Surface character	Mildly acidic, zeta potential ~ -60 mV at pH 7[a]	Basic, zeta potential $\sim +30$ mV at pH 7[a]
Able to engage in acid–base-type secondary bonding with	Basic functionality on a polymer	Acidic functionality on a polymer

[a] Degussa technical bulletin Pig. 11-7-105-893 DD.
[b] Measured by us.

acidic silica substrate, and aluminum oxide C or ALOC™ (Degussa AG), as a model basic adsorbent. Both substrates were supplied as ~1-μm particles with a negligible internal pore structure. As such, the polymer was assumed to be adsorbed onto an approximately flat surface with a surface area similar to that measured by the BET experiment,[98] 110 m^2/g for Aerosil 130 and 88 m^2/g for ALOC. The characteristics of both adsorbents are summarized in Table II.

Solvent quality with respect to the styrene segment was varied from "good" to theta (θ) quality using carbon tetrachloride (CCl_4, $\chi = 0$ at 35°C) or cyclohexane (CH, $\chi = 0.5$ at 35°C), respectively. Neither solvent is a displacer of styrene segments from either of Aerosil 130 or ALOC, and so end-cap functionality competes for surface sites on the substrate with in-chain segments of the polymer.

Equilibrium-adsorbed levels of the polymer were determined using the "depletion" method outlined earlier, through insertion of SA = 110 m^2/g for Aerosil 130 and 88 m^2/g for the ALOC adsorbent into the appropriate equation. Adsorption isotherms were all of the high-affinity type.[79] The equilibrium-adsorbed amount of the polymer (Γ, mg/m^2) was determined as an average of the data points collected over the plateau region of the adsorption isotherm. As an example of the utility of this simple experiment, we sketch in Figure 5 the adsorption isotherms for polymer A3 (M_n = 40 kD, COOH-terminated) onto ALOC from CH (open diamonds) and from CCl_4 (filled diamonds) at 35°C. For this polymer, decreasing the solvent quality from $\chi = 0$ (CCl_4) to $\chi = 0.5$ (CH) and increasing the segment–surface interaction parameter (χps) from ~1 kT (CCl_4) to ~2 kT (CH) more than doubles the equilibrium-adsorbed amount onto ALOC at this temperature.

Γ: Theoretical Predictions and Experimental Verification

SCF-type computer simulations, as detailed previously, yield valuable insight into the equilibrium state of polymers adsorbed onto interfaces from a dilute solution. However, the method possesses some limitations, the most important of which derives from a relationship between the chain length (N) and computational time, which currently limits us to a maximum (of convenience) at about $N = 200$. No such limitation is observed experimentally, and we may prepare for examination polymers covering a wide range of chain lengths. In contrast, the SCF method allows us to fix all adsorption parameters but one (of N, χ, χps,

Δ) which may be varied continuously, yielding a relationship between Γ and that variable. This can be difficult to achieve by experiment, as all parameters become interrelated. For example, if we change the polymer segment (e.g., from styrene to methyl methacrylate) to vary χps, we also change the solvent power (χ). *More importantly,* if the solvent is changed to vary χ, χps changes also. We see, therefore, that experimental observation can be used to test the validity of the SCF calculations, that SCF calculations may be used to predict experimental outcomes, and that situations exist which may be probed by only one method. In this section, we explore the relationships among N, χ, χps, Δ, and Γ, the equilibrium-adsorbed amount of the polymer at the interface. Some representative SCF adsorption simulations are summarized in Figure 6. Experimentally measured surface excesses of the polymers onto Aerosil 130 and onto ALOC from CH and from CCl_4 at 35°C are given in Table III.

χ and χps: Solvent Quality and the Segment–Surface Interaction Parameter

As expected, *in the absence of end-group functionality* ($\Delta - \chi ps = 0$, Fig. 6, left—top and bottom, $x = 0$), *SCF calculations* predict that $\Gamma \rightarrow 0$ when $\chi ps \rightarrow 0$. Increasing χps from 0.1 to 1.0 kT at a constant chain length (N) and solvent quality (χ) enormously increases polymer adsorption (Γ). Adsorption from a nondisplacing theta ($\chi = 0.5$) solvent is enhanced over that from a nondisplacing good ($\chi = 0$) solvent at constant N and χps.

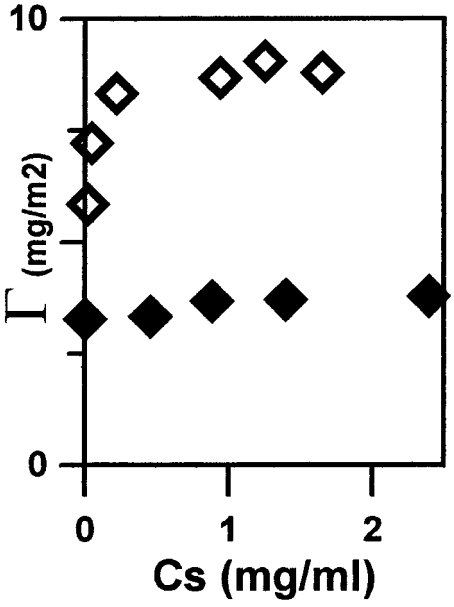

Figure 5 Equilibrium-adsorbed mass (Γ, mg/m^2) of carboxylic acid-terminated polymer (M = 40 kD) onto ALOC (open diamonds) from cyclohexane and (filled diamonds) from carbon tetrachloride at 35°C versus equilibrium solution concentration (C, mg/mL).

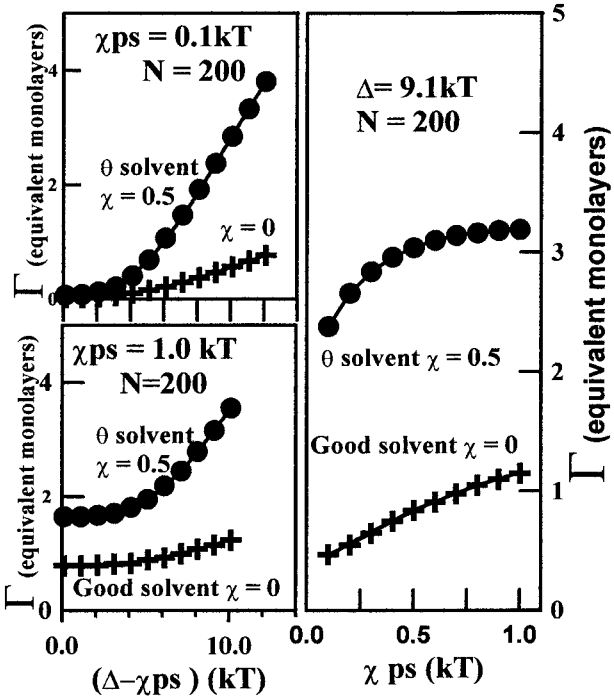

Figure 6 SCF calculations plotted to elucidate the dependence of Γ on χps and on Δ, for a chain of length N = 200, adsorbed from a theta solvent (χ = 0.5) and from a good solvent (χ = 0). (Top left) χps fixed at 0.1 kT, with changing $\Delta - \chi ps$. (Bottom left) χps fixed at 1.0 kT, with changing $\Delta - \chi ps$. (Right) Δ fixed at 9.1 kT, with changing $\Delta - \chi ps$. (Data points have been omitted for clarity of presentation.)

If we compare the *experimentally observed* adsorption amounts, measured for *nonfunctionalized polystyrenes* (Table III, PS-[7-400]), from a nondisplacing good solvent (CCl_4, $\chi = 0$) and from a nondisplacing theta solvent (CH, $\chi = 0.5$) onto Aerosil 130 and onto ALOC, it becomes clear for a fixed solvent (χ) and adsorbent (χps) that Γ increases with the molecular weight of the polymer. If chain length (N) and absorbent are now fixed, adsorption from the theta solvent (CH) is measured to be greater than from the good solvent (CCl_4) as predicted by SCF theory (above). [Note: The experimentally measured $\chi ps \sim F$(solvent structure), so this changes $\sim F(d(\chi)\ and\ d(\chi ps)$]. If we now allow the chain length to vary onto a fixed substrate, this difference ($d\Gamma = \Gamma\theta - \Gamma$good) is

Table III Equilibrium Surface Excess (Γ) of Polymer onto Acidic and Basic Substrates

	Γ (mg/m^2) onto Aerosil 130 at 35 ± 0.1°C		Γ (mg/m^2) onto ALOC at 35 ± 0.1°C	
Polymer	From CCl_4	From Cyclohexane	From CCl_4	From Cyclohexane
A1	0.83	1.60	2.84	5.08
A2	0.99	1.94	3.68	6.32
A3	0.98	2.20	3.79	8.75
A4	1.29	3.16	3.50	10.40
A5	1.33	3.19	2.89	9.42
B1	0.72	1.68	0.75	1.70
B5	1.14	2.75	0.83	4.66
C1	0.62	1.30	0.61	1.37
C5	0.99	2.38	0.68	2.73
D1	1.34[a]	4.45	1.21	3.37
D2	1.39	4.70	1.24	3.51
D3	1.38	4.98	1.29	3.57
D4	1.65	5.78	1.49	4.22[a]
D5	1.73	6.82	1.57	4.83
D-6 kD	1.24[a]	3.97[a]	1.12[a]	3.01[a]
D-300 kD	1.73[a]	6.63[a]	1.57[a]	4.71[a]
PS-7	0.61	1.08	0.32	0.98
PS-50	0.72	1.46	0.55	1.25
PS-200	0.98	2.35	0.65	2.22
PS-400	1.05	2.57	0.76	2.56
PS-6 kD	0.58[a]	1.01[a]	0.33[a]	0.88[a]
PS-300 kD	1.01[a]	2.44[a]	0.73[a]	2.33[a]

[a] Calculated from the best-fit straight line to a plot of ln Γ versus ln M_n.

shown to increase with the molecular weight of the polymer. The segment–surface interaction parameter for polystyrene onto silica from CCl_4 and from CH was measured previously as ~1 and ~2 kT, respectively.[38,41] By noting that Γ(Aerosil 130) > Γ(ALOC) for a fixed chain length and solvent, and through comparison of the adsorbed amounts, it can be inferred, qualitatively, that χps for polystyrene onto ALOC from CCl_4 is significantly less than ~1 kT and that χps for polystyrene onto ALOC from CH is slightly less than ~2 kT.

SCF computer simulations allow us to isolate, for examination, the influence of changes in the segment–surface interaction parameter (χps) only, on the equilibrium surface excess *when a single polymer end cap interacts strongly with the surface*. As an example, we sketched in Figure 6 (right) the dependence of Γ on χps at a fixed chain length (N = 200) and solvent quality χ, when Δ = 9.1 kT. At this extreme of a large Δ, a substantial amount of polymer is deposited onto the surface from both a good and a theta solvent even when $\chi ps \rightarrow 0$. Deposition from the theta solvent is enhanced over that from the good solvent at fixed χps throughout the interval $0 < \chi ps < 1$. As $\chi ps \rightarrow 1$, adsorption from the theta solvent appears to "plateau out" at N = 200 and Δ = 9.1 kT. In contrast, adsorption from the good solvent continues to rise monotonically throughout this interval, but to remain much reduced over that calculated for the theta solvent.

Δ: The Polymer End Cap–Surface Interaction Parameter

The variance of Γ with Δ at a fixed chain length (N = 200), solvent quality (χ = 0 or 0.5), and segment–substrate interaction parameter (χps = 0.1 or 1.0), *as calculated by SCF*, is summarized in Figure 6 (left, top, and bottom). In the limit of weak segment–surface interactions (χps = 0.1), Γ increases with Δ from a limiting value of Γ ~ 0 at Δ = χps = 0.1 to a high adsorbance when the end

cap interacts strongly with the surface. Upon fixing the segment–surface interaction at a level closer to that measured for polystyrene onto an inorganic substrate from a nondisplacing solvent (χps = 1.0), the surface excess increases from a moderate to high level with increasing Δ over the measured range of Δ's. Irrespective of the magnitude of χps within the range 0.1–1.0, adsorption of an end-capped polymer (with $\Delta > \chi ps$) from a theta solvent at fixed χps exceeds that from a good solvent by a wide margin, which increases with Δ. (At increasing Δ, the internal polymer segments contribute less to the overall adsorption of polymer.) In other words, *the magnitude of the surface-adsorbed amount* (Γ) *is a diminishing function of* χps *at increasing* Δ. For example, if we extrapolate the calculated adsorption curves from a theta solvent as a function of Δ at the two extremes of χps, we may predict a crossover at ($\Delta - \chi ps$) $\sim$ 16 kT, after which the system characterized by a lower χps yields a larger adsorbed amount. The position of this crossover point is obviously a function of the two values of χps used to construct the Γ versus ($\Delta - \chi ps$) curves. Ignoring kinetic effects, at the limit of $\chi ps \rightarrow 0$ & $\Delta \gg$ 9.1 kT, the equilibrium-adsorbed amount reflects a balance between the energy released when the end group displaces a solvent molecule from the surface and the drop in entropy associated with tethering, then extending the chain in the z direction. If χps is now "turned on" ($0 < \chi ps \ll \Delta$), the end group and more numerous chain segments close to the surface must compete for surface sites with sticking probabilities $\sim e^{-\Delta}$ and $\sim e^{-\chi ps}$, respectively. Fixing Δ and increasing χps so that $0 \ll \chi ps \ll \Delta$, will increase the segment density at the surface, enhancing both the entropy penalty and the diffusional barrier which must be overcome by incoming chains to reduce Γ (and vice versa).

Some of these predictions may be verified by reference to the *measured equilibrium-adsorbed amounts of the polymer* summarized in Table III. (We may assume throughout that χps for the adsorption of these polystyrenes onto Aerosil 130 from CCl_4 is about 1 kT, that χps for the adsorption of these polystyrenes onto Aerosil 130 from cyclohexane is about 2 kT, and that χps for the adsorption onto ALOC from CCl_4 and from cyclohexane is somewhat less than 1 and 2 kT, respectively). For instance, it may be verified by calculation for any of the end-capped polymers (by fixing χps, Δ, and N) that adsorption of a polymer from a theta solvent onto a surface generates a larger adsorbed amount than does adsorption of that same polymer from a good solvent onto that surface. If we compare the adsorption of polymers with similar molecular weights but possessing differing end cap–surface interaction parameters (Δ) onto the same surface from the same solvent (fixing χ, χps, and N), we find that Γ is an increasing function of Δ. (For example, Δ[A1] > Δ[B1] > Δ[C1], while Γ[A1] > Γ[B1] > Γ[C1], where A1: COOH, B1: OH, and C1: $COOCH_3$). If we consider *qualitatively* the combined influence of the molecular weight and solvent quality on the adsorption of otherwise identical polymers onto a fixed substrate, we find that the equilibrium-adsorbed amount of the polymer adsorbed from a theta solvent (CH, χ = 0.5) onto a substrate is both a larger and a stronger function of molecular weight than is the equilibrium-adsorbed amount of the same polymer adsorbed from a good solvent (CCl_4, χ = 0). We must, however, temper this conclusion with the observation that both χps *and* Δ are solvent-dependent in real systems, and so the observed trend may not be assigned uniquely to changes in any one of χ, χps, or Δ.

N: Chain Length

Previously, we touched qualitatively upon the influence of chain length (N) on the surface excess (Γ). It was observed elsewhere[79,118] that the equilibrium surface excess of the linear homopolymer adsorbed onto a surface often scales as $\Gamma \sim M^a$ (or $\sim kN^a$, with $k \sim Mo^a$), where M is the chain mass; N, the chain length; and Mo, the repeat unit mass, and a is usually assumed as an invariant number which defines a relationship between chain length and surface excess. The magnitude of a, as a marker of molecular weight dependence, may be determined by graphing experimentally measured or calculated values of Γ against M or N as ln{Γ} as y versus ln{M or N} as x and extracting a as the instantaneous gradient of the scatter plot so obtained. The variance of a as a function of N or M gives a numerical measure of the relationship between Γ and M or N and how that relationship is perturbed by Δ. For example, if a is positive, large, and invariant, Γ becomes a strong and increasing function of N over the defined range of N. A similar effect may be achieved if a is small but increases over the defined range of N. If a decreases over the defined range of N, even if large throughout, Γ may become a weak or even a decreasing function of N, etc.

Equilibrium SCF calculations for Γ were performed from a lower limit of $N = 100$ to an upper limit of $N = 300$ (for convenience). For a polystyrene polymer, this would correspond to an upper mass of ~31,000 D. Our experimental and computational estimates of a are, therefore, complimentary with some overlap. Most of the SCF calculations for a as a function of N, χ, χps, and Δ are summarized in Figure 7. In all the modeled systems, a was calculated as a changing function of N.

In the absence of an end cap ($\Delta = 0.1$ kT, bottom chart, Fig. 7), adsorption of both a weakly interacting ($\chi ps = 0.1$ kT) or a strongly interacting ($\chi ps = 1.0$ kT) polymer from either of a theta ($\chi = 0.5$) or a good ($\chi = 0$) solvent produces a relatively invariant positive exponent, indicating that surface excess is an increasing function of N over the studied range of N. Over the entire range of N, and from either of a theta or a good solvent, the equilibrium adsorption (Γ) of *weakly interacting polymer* with the surface ($\chi ps = 0.1$ kT, #1 and #3) is a much stronger function of N (larger a) than is the adsorption of a more strongly interacting polymer ($\chi ps = 1.0$ kT, #2 and #4) from that solvent. [For example, if $\chi = 0$, $\chi ps = 0.1$, and $\Delta = 0.1$, $\Gamma_{300} \sim 2.27\Gamma_{100}$, whereas if $\chi = 0$, $\chi ps = 1.0$, & $\Delta = 0.1$, $\Gamma_{300} \sim 1.38\Gamma_{100}$ ($2.27 > 1.38$, etc.)] The same calculation for adsorption from a theta solvent would yield a similar result, for example, for adsorption from a theta solvent, $\Gamma_{300} \sim 1.9\Gamma_{100}$ when $\chi ps = 0.1$ and $\Gamma_{300} \sim 1.11\Gamma_{100}$ when $\chi ps = 1.0$. In addition, the adsorption of *weakly interacting polymer* ($\chi ps = 0.1$ kT) from a good solvent (#3) is predicted as a stronger function of N (larger a) than is the corresponding adsorption from a theta solvent (#1)—compare the coefficients 2.27 and 1.9 above. For *a more strongly adsorbing polymer* ($\chi ps = 1.0$ kT), the reverse holds at short chain lengths at which adsorption from a theta solvent (#2) is a stronger function of N (larger a) than is adsorption from a good solvent (#4). As chain length increases to $N = 300$, the variance of Γ on N (a), for $\chi ps = 1.0$ kT from either of a good or a theta solvent (#4 and #2, respectively), appears to converge to a common value. (We must perform these calculations at longer N to determine if we are witness to a convergence or crossing of these two curves.) Over the entire range of N, however, adsorption from the good solvent is a stronger function of chain length than is adsorption from a theta solvent, as evidenced by $\Gamma_{300} \sim 1.38\Gamma_{100}$ for adsorption from the good solvent, while $\Gamma_{300} \sim 1.11\Gamma_{100}$ from the theta solvent.

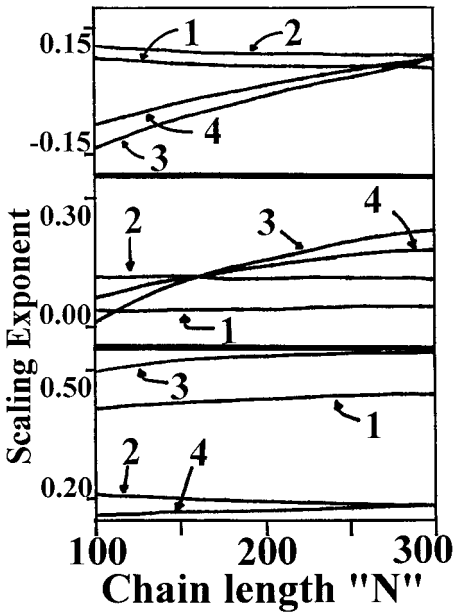

Figure 7 ($\Gamma \sim N^a$). Plots of a (exponent) versus N (chain length) by SCF for (top) $\Delta = 20$ kT, (middle) $\Delta = 9.1$ kT, and (bottom) $\Delta = 0.1$ kT. (1) θ solvent, $\chi = 0.5$, $\chi s = 0.1$ kT; (2) θ solvent, $\chi = 0.5$, $\chi s = 1.0$ kT; (3) good solvent, $\chi = 0$, $\chi s = 0.1$ kT; (4): good solvent, $\chi = 0$, $\chi s = 1.0$ kT.

In the presence of a *strongly interacting end cap* ($\Delta = 9.1$ kT, middle chart, Fig. 7), all exponents (a) remain positive over the studied range of N so that Γ is an increasing function of N over the range $100 \leq N \leq 300$. Even so, the end cap is shown to modify, fundamentally, the adsorption event. For example, if deposited from a *theta solvent*, the adsorption of the polymer with more strongly adsorbing segments ($\chi ps = 1.0$ kT, #2, larger a throughout) would seem to be a significantly stronger function of N over the entire studied range than is the adsorption of polymer with less strongly adsorbing segments ($\chi ps = 0.1$ kT, #1, smaller a throughout). However, small *changes* in the a values throughout this range of N nullify this difference, so that $\Gamma_{300} \sim 1.11\Gamma_{100}$ for both sets of polymers. The end cap (with $\Delta = 9.1$) would, therefore, appear to reduce the molecular weight dependence of the adsorption from a theta solvent over the range $0.1 \leq \chi ps \leq 1.0$. For adsorption of a polymer from a *good solvent*, the exponent a is now a strongly increasing function of N at both extremes of χps. At $N \sim 100$, the adsorption of a polymer with more strongly adsorbing segments ($\chi ps = 1.0$ kT, #4) appears to be

a stronger function of N (larger a) than is adsorption of a polymer with less strongly adsorbing segments (χps = 0.1 kT, #3). As N increases, the situation reverses and the adsorption of a polymer with less strongly adsorbing segments (χps = 0.1 kT) becomes the stronger function of N. Over the entire range of N, however, the adsorbance of a polymer with less strongly adsorbing segments remains a stronger function of N ($\Gamma_{300} \sim 3.46\Gamma_{100}$ for χps = 0.1) than is adsorption of the polymer with more strongly adsorbing segments ($\Gamma_{300} \sim 2.5\Gamma_{100}$ for χps = 1.0).

If the *end cap–substrate interaction parameter* is further increased (Δ = 20 kT, upper chart, Fig. 7), some striking trends become evident: All four exponents a become changing functions of N. Over the entire range of N, the adsorption of a polymer from a *theta solvent* (Fig. 7, top, #1 & #2) is characterized by a positive (although monatonically decreasing) exponent. Over the entire range of N, the adsorption of a polymer with more strongly interacting segments (χps = 1.0 kT, #2) is characterized by a larger exponent (a) than is the adsorption of a polymer with less strongly adsorbing segments (χps = 1.0 kT, #1) However, *changes* in a values result in marginal drops in adsorption over this chain length interval for both types of polymer. For example, $\Gamma_{300} \sim 0.97\Gamma_{100}$ for χps = 0.1 kT, while $\Gamma_{300} \sim 0.98\Gamma_{100}$ for χps= 1.0 kT. In contrast, the adsorption of a polymer from a *good solvent* (Fig. 7, top, #3 and 4) is characterized by strongly increasing exponents a throughout the entire range of N. At low N, the adsorption of the polymer with less strongly interaction segments (χps = 0.1 kT, #3) is characterized by the largest $|a|$. At longer N, both exponents become positive and appear to converge to a common value at N = 300. (Again, we must perform these calculations at longer N to determine if we are witness to a convergence or crossing of these two curves.) Over the entire range of N, the adsorption of a more weakly interacting polymer (χps = 0.1 kT, #3, $\Gamma_{300} \sim 2.9\Gamma_{100}$) remains a stronger function of the molecular weight than is adsorption of a more strongly interacting polymer (χps = 1.0 kT, #4, $\Gamma_{300} \sim 2.3\Gamma_{100}$).

In summary, therefore, SCF calculations predict that *in the absence of an end cap*, and at a fixed solvent quality (χ), the molecular weight dependence of Γ is "inversely" related to χps. If χps is fixed, the equilibrium-adsorbed amount (Γ) becomes a stronger function of N from a good solvent than from a theta solvent. *Increasing* Δ ($0.1 \rightarrow 9.1 \rightarrow 20$) reduces and converges the molecular weight dependence of Γ from a *theta solvent* at both extremes of χps (0.1 and 1.0), to suggest that the equilibrium adsorption (Γ) may become an inverse function of N. In other words, if σ = the number of chains/unit surface and N = the chain length, at sufficiently large $\Delta \gtrsim 20$, σ_l. $N_l > \sigma_h$. N_h, with l = low, h = high, etc. The influence of increasing Δ on the adsorption of a polymer from a *good solvent* is more difficult to define. In all three systems, fixing Δ at 0.1, 9.1, and 20 kT results in a molecular weight dependence of Γ which is inversely related to χps. If χps is fixed, the molecular weight dependence of Γ, over the range $100 \leq N \leq 300$, first increases (Δ = 9.1) and then decreases (Δ = 20). *Clearly, the molecular weight dependence of* Γ *for an end-functionalized polymer remains a strong function oft solvent quality over this molecular weight interval*.

Turning now to observations on experimentally gathered data, we summarize in Table IV trends in the experimentally determined values of Γ as a function of M or N. Throughout, we examine the "goodness of fit" of the data to the relationship $\Gamma \sim kM^a$ with invariant a from the correlation coefficient of a plot of $\ln\{\Gamma\}$ as y versus $\ln\{M\}$ as x. Table IV contains a listing of a and $\ln k$ values and correlation coefficients (R) to an attempted linear fit for the adsorption of nonfunctional (PS–H), carboxylic acid-terminated (PS–COOH, Series A), and dimethylamino-terminated [PS–N$(CH_3)_2$, Series D] polymers onto Aerosil 130 and onto ALOC from carbon tetrachloride (CCl_4) and from cyclohexane (CH). In the following discussion, we assume that adsorption onto Aerosil 130 from CCl_4 is characterized by $\chi ps \sim 1.0$ and that adsorption onto ALOC from CCl_4 is characterized by $0.1 < \chi ps < 1.0$. We also assume that adsorption onto Aerosil 130 from CH is characterized by $\chi ps \sim 2.0$ and that adsorption onto ALOC from CH is characterized by $1 \lessapprox \chi ps < 2.0$. As expected, from examination of the correlation coefficients, the relationship $\Gamma \sim kM^a$ is better fit by considering M as the number-average molecular weight (M_n) than as the weight-average molecular weight (M_w). The adsorption of all polymers from both solvents onto Aerosil 130 adheres to a power law fit in M_n of the type $\Gamma \sim {M_n}^a$ with an invariant positive coefficient a over the studied interval, as does the adsorption of PS–H and Series D polymers from both solvents onto ALOC, resulting in equilibrium-adsorbed amounts which are increasing functions of M, as predicted by SCF for $\Delta \leq 20$. We cannot reconcile the invariance of a on

M (or N) as revealed by experiment at higher N with the strong dependence of a on N in some instances as revealed by SCF at lower N, except to mention that calculated values of $da/dN \rightarrow 0$ as $N \rightarrow 300$ for most systems (Fig. 7), which could lead to an invariant a at higher N. In contrast, the very strong end-group interaction between the carboxylic acid-terminated Series A polymers and ALOC leads to pronounced curvatures in the plots of ln{Γ} as y versus ln{M} as x from both solvents, which result in a nonlinear increase and then a decrease in Γ with increasing M. (In the vocabulary of the preceding section, the numerical value of a first increases at low M to a positive turning point, then drops through zero to a negative turning point at high M.)

Previous SCF-type calculations (above) have suggested that Γ may be represented as a decreasing function of N at sufficiently high Δ. Even so, we lack, at this point, sufficient insight to explain this more complex experimental trend. Assuming continued linearity in plots of ln{Γ} versus ln{M} at low M, the influence of end-cap functionality on Γ could be isolated through comparison of ln k values, with ln k as an expected increasing function of Δ. However, we have indicated previously by SCF calculations that a may become a strong function of N at the limit $N \rightarrow 0$. Nonetheless, the measured values of ln k track the expected ordering of Δ when ln{Γ} can be measured as a linear function of ln{M}. For example (Table IV), if we consider adsorption onto Aerosil 130 from either CCl_4 or cyclohexane (CH), ln k(Series D) > ln k(Series A) > ln k(PS–H), as expected. If χps is solvent-dependent, then Δ must also be a function of the solvent structure. If we assume that values of Δ and ln k scale accordingly, the measured values of ln k suggest that $\Delta_{CH} > \Delta_{CCl4}$ for adsorption onto Aerosil 130 when $\Delta > \chi ps$. Identical observations may be made for adsorption onto ALOC.

Trends in polymer adsorption versus M over the studied interval are summarized visually in Figure 8. *In the absence of an end cap* (PS–H) and onto a fixed surface, it can be seen that the equilibrium-adsorbed amount at corresponding M is greater from the theta solvent than from the good solvent, as predicted by SCF theory. This comparison is, of course, complicated, in that, for these real systems, χ and χps are convoluted as outlined above, leading to an increase of χps from the "good" [$\chi ps \sim 1$ kT] to the theta [$\chi ps \sim 2$ kT] solvent onto silica, resulting in an additive influence on Γ. In contrast, however, the equilibrium

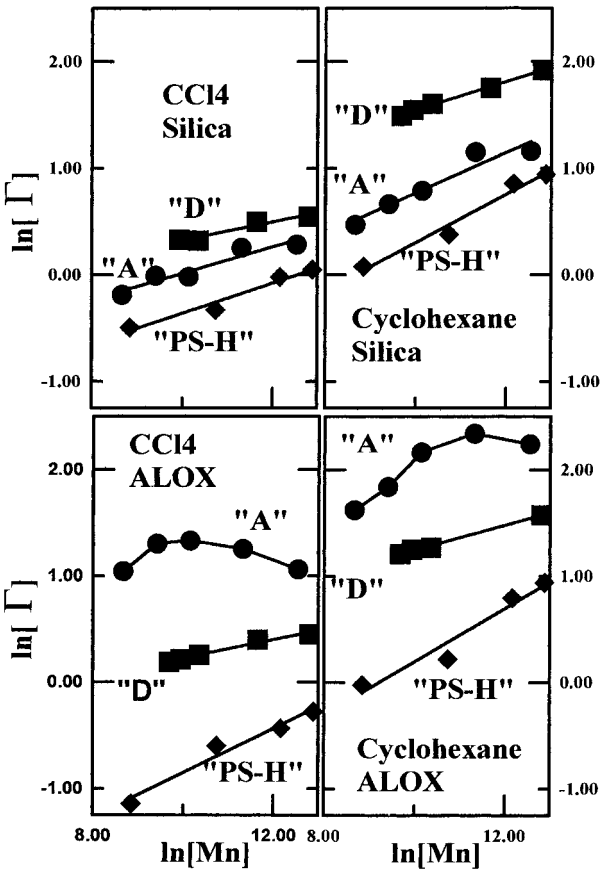

Figure 8 Plots of ln[Γ] versus ln[M_n] from the indicated solvent to the indicated adsorbent at 35°C. Nonfunctionalized polystyrenes are designated as PS–H. Series A polymers are terminated with COOH functionality. Series D polymers are terminated with the —N(CH3)2 functional group.

adsorbance (Γ) is shown also to be a stronger function of M (larger a) from this theta solvent than from this good solvent onto the same substrate. The results of the SCF calculations (above) would suggest the opposite: that the additive influence of changing χ from 0 to 0.5 and χps from ~ 1.0 to ~2.0 should reduce the molecular weight dependence of Γ. Clearly, further SCF calculations at higher N should be performed to resolve this discrepancy.

The influence of χ and χps on Γ may be factored out by fixing the solvent and substrate, allowing for an investigation of the influence of Δ on the equilibrium adsorption (Γ). In choosing CCl_4 as the solvent and Aerosil 130 as the substrate (Fig. 8, top left), it becomes obvious, for these real systems, that increasing Δ (PS–H → A → D) increases Γ at fixed M, χ, and χps and that increasing Δ reduces a and, therefore, the molecular

weight dependence of Γ at fixed χ and χps. The same inferences may be made through consideration of the adsorption of these polymers from CH onto Aerosil 130 (Fig. 8, top left) and from CCl_4 and CH onto ALOX (Fig. 8, bottom left and right, respectively).

Estimating Δ

We (and others) have shown that the enthalpic interaction between in-chain polymer segments and the surface, quantified as χps, the surface–segment interaction parameter, influences profoundly the equilibrium-adsorbed amount or Γ. Methods for the determination of χps have been determined.[101–103] In contrast, the experimental determination of Δ, the end cap–surface interaction parameter, is more problematic. We have undertaken to develop a method for the determination of Δ for a single-end-functionalized polymer, for which χps has been determined previously. With reference to Figure 6, it would seem that a knowledge of Γ, χ, χps, and N would allow for a direct determination of Δ. Unfortunately, the translation between the calculated surface-adsorbed amount (Γ, equivalent monolayers) and the measured surface-adsorbed amount (Γ, mg/m^2) is not trivial and involves some assumptions. The equating of these two measurements is more easily undertaken if both could be made dimensionless. This is most easily undertaken by establishing ratios of the type $\Gamma x/\Gamma_H$. Here, Γ_H = the surface excess for a homopolymer of degree N, from a solvent characterized by χ, onto a surface characterized by $\Delta = \chi ps$, while Γx = the surface excess for the single-end-capped homopolymer of identical N, from the same solvent, and onto the same surface, where x is characterized by $\Delta > \chi ps$. Both experimental and calculated values of Γ are determined for solutions below the critical overlap concentration (c^*) at which Γ is only a weak function of c. If we assume, therefore, that calculated and measured ratios can be equated, then the end-cap–surface interaction parameter may be determined from plots of calculated $\Gamma x/\Gamma_H$ versus Δ at fixed N, χ, and χps, by correlating an experimentally measured $\Gamma x/\Gamma_H$ ratio with the corresponding value of Δ. Intuitively, we would predict that the ratio $\Gamma x/\Gamma_H$ would increase with Δ at fixed N, χ, and χps. We would also predict that the ratio $\Gamma x/\Gamma o$ would scale as some inverse function of N at fixed χ, and χps, as the influence of the chain end is diluted at larger N.

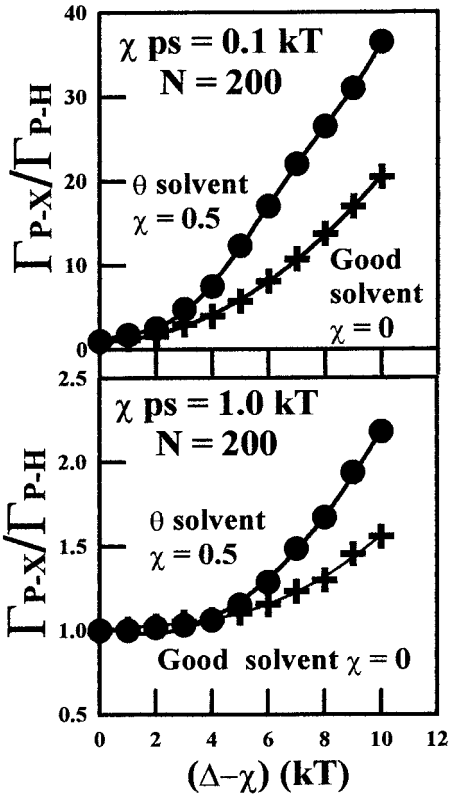

Figure 9 SCF calculations plotted to elucidate the dependence of the dimensionless ratio ΓP–X/ΓP–H, for a chain of length N = 200, adsorbed from a theta solvent (χ = 0.5) and from a good solvent (χ = 0) as a function of Δ. (Top) χps fixed at 0.1 kT. (Bottom) χps fixed at 1.0 kT. (Data points have been omitted for clarity of presentation.)

The results of SCF calculations quantifying the influence of χ, χps, and Δ on $\Gamma x/\Gamma_H$ at N = 200 are sketched in Figure 9. At fixed Δ, the ratio $\Gamma x/\Gamma_H$ scales inversely with χps, in the range $0.1 \leq \chi ps \leq 1.0$ (In other words, a fixed end cap is more effective at enhancing adsorption when the in-chain polymer segments interact less strongly with the surface.) At fixed χps, the ratio $\Gamma x/\Gamma_H$ increases with $(\Delta - \chi ps)$ throughout the range $0.1 \leq (\Delta - \chi ps) \leq 12$ (In other words, a more strongly adsorbing end group is more effective at enhancing adsorption of the polymer.) At fixed χps and Δ, the ratio $\Gamma x/\Gamma_H$ scales inversely with χ in the range $0 \leq \chi \leq 0.5$. (In other words, a fixed end cap is more effective at enhancing the adsorption from a theta solvent than from a good solvent onto a fixed surface.)

To illustrate the influence of a more strongly adsorbing end cap on the adsorption process, we chose to compare in a bar chart (Fig. 9) $\Gamma x/\Gamma_H$

Table IV Summary of Equilibrium ln{Γ} versus ln{mass} Plots for Polymers onto Aerosil 130 and onto ALOC from Carbon Tetrachloride and from Cyclohexane

$\Gamma \sim kM^a$ Data is Tabled as a R ln k (R = Correlation Coefficient)		Equilibrium Adsorption onto Aerosil 130 at 35 ± 0.1°C				Equilibrium Adsorption onto ALOC at 35 ± 0.1°C			
		From CCl_4		From Cyclohexane		From CCl_4		From Cyclohexane	
		Mass Average							
		M_n	M_w	M_n	M_w	M_n	M_w	M_n	M_w
Polystyrene standards PS–H	a	0.1411	0.979	0.2258	0.984	0.2076	0.986	0.2495	0.969
	R	0.981		0.986		0.984		0.973	
	ln k	−1.772		−1.954		−2.925		−2.297	
	Γ	$\Gamma \sigma kMn^a$		$\Gamma \sigma kMn^a$		$\Gamma \sim kMn^a$		$\Gamma \sim kMn^a$	
A Series PS–COOH	a	0.124	0.119	0.1895	~0	0.137	0.687	0.861	0.317
	R	0.954		0.961		$\Gamma \not\sim kMn^a$		$\Gamma \not\sim kMn^a$	
	ln k	−1.226		−1.126					
	Γ	$\Gamma \sim kMn^a$		$\Gamma \sim kMn^a$					
D Series PS–$N(CH_3)_2$	a	0.864	0.946	0.1315	0.996	0.0872	0.986	0.1238	0.999
	R	0.966		0.998		0.988		0.999	
	ln k	−0.540		0.234		−0.646		0.102	
	Γ	$\Gamma \sim kMn^a$		$\Gamma \sim kMn^a$		$\Gamma \sim kMn^a$		$\Gamma \sim kMn^a$	

values for the four end-cap functionalities available to us: for polymer adsorbed from cyclohexane and from carbon tetrachloride onto Aerosil 130 and onto aluminum oxide C, at M_n = 6 kD and 300 kD. Some adsorbed amounts (Γ, mg/m^2) used in the calculation of $\Gamma x/\Gamma_H$ values were estimated from linear least-squares best-fit straight lines through the appropriate plot of ln[Γ] versus ln[M_n] (Fig. 8 and Table IV), as annotated (*) in Table III. As expected, the end cap exerts a stronger influence on the adsorption process at 6 kD than at 300 kD. Onto both Aerosil 130 and ALOC, the relative influence of the end-cap functionality tracks the measured R_f values measured in the preliminary TLC experiments as $\Gamma \sim F[1/Rf]$ and the ln k values as discussed in the previous section as $\Gamma \sim F[\ln k]$. The opportunity for acid–base interactions between the end cap and the surface (acidic Aerosil 130, basic Series D polymers; basic ALOC, acidic Series A polymers) increases enormously the measured dimensionless surface excess ratio. A single ester end group appears singularly ineffective in enhancing adsorption onto silica and only slightly more effective at enhancing adsorption onto ALOC, while a single hydroxyl functionality is only marginally more effective onto both surfaces. For adsorption of M_n = 6 kD polymers onto Aerosil 130, it is noted that the end cap is significantly more effective at enhancing the adsorption of all the end-functionalized polymers from the θ solvent (cyclohexane) than from the good solvent (CCl_4), as predicted from the SCF calculations outlined here. (As mentioned previously, changing the solvent influences χ, χps, and Δ for real polymer/solvent systems.) In contrast, for adsorption of these same M_n = 6 kD polymers onto ALOC, we find, with the exception of the secondary amine-terminated polymer [X = $N(CH_3)_2$], that the normalized adsorption of low mass ester, hydroxyl, and carboxylic acid-terminated polymers is more significantly enhanced from the good solvent than from the theta solvent, in opposition to the trend predicted by the SCF calculations. We may surmise, as a possible explanation for this discrepancy, that Δ for Series A polymers onto ALOC may be sufficiently large as to introduce an element of irreversibility into the adsorption process. However, this argument cannot hold for the less strongly adsorbing Series B, C, and D polymers onto ALOC. Clearly, more investigations are required to resolve this anomaly.

We propose that an estimate for Δ may be retrieved from a plot of $\Gamma x/\Gamma_H$ versus Δ which has been constructed by SCF calculation using appropriate values for χ, χps, and N. We would simply

read from the graph the x value (Δ) which corresponds to the experimentally measured y value ($\Gamma x/\Gamma_H$). If we are to use ($\Gamma x/\Gamma_H$ values corresponding to a polystyrene chain of mass 6 kD, a value of $N \sim 60$ must be entered into the calculations. For a theta solvent (cyclohexane at 35°C), $\chi = 0.5$; for a "good" solvent (CCl_4 at 35°C), $\chi = 0$. The polymer segment–surface interaction energy (χps) measures the preferential enthalpy of adsorption of a polymer segment over a solvent molecule onto the surface and was estimated for polystyrene onto a silica surface as $\chi ps \sim 1.0$ from CCl_4 and ~ 2.0 from cyclohexane at 35°C.[38,41] From graphs of the calculated $\Gamma x/\Gamma_H$ ratios versus Δ, as constructed for adsorption under conditions which simulate the behavior of both solvents onto silica, we may establish values of Δ for the end group. A plot of calculated $\Gamma x/\Gamma_H$ ratios versus Δ under these constraints, as reproduced in Figure 11 for adsorption from the simulated theta solvent (top) and from the simulated good solvent (bottom), is decidedly nonlinear at low Δ and monotonically increasing at higher Δ. The influence of the polymer concentration on the enhanced adsorption is illustrated through the inclusion of scatter plots for adsorption from 0.1, 1.0, and 5.0% polymer solutions. It may be observed from both solvents and over the studied ranges of Δ that the extent to which end-group functionality (with $\Delta > \chi ps$) enhances the equilibrium-adsorbed amount is inversely related to the polymer concentration in the solution. This effect diminishes for adsorption from a good solvent at higher values of Δ and, in fact, becomes reversed for adsorption from a theta solvent at $20 \sim \Delta \sim 22$.

Raw data to calculate the ratios ($\Gamma x/\Gamma_H$) was collected from high-affinity adsorption isotherm plateaus corresponding to $c \sim 0.1\%$, and so estimates of Δ for carboxylic acid and dimethylamino end caps were obtained from polynomial fits to scatter plots at that concentration. By these means, the enthalpy of adsorption of a carboxylic acid end cap from carbon tetrachloride onto activated Aerosil 130 silica (Δ) was estimated as ~8.2 kT (with χps ~1.0 kT) and from cyclohexane onto activated Aerosil 130 silica (Δ) as ~9.9 kT (with χps ~2.0 kT). Both values of Δ lie within the boundaries of previous experimentation.[39] As expected, changes in the magnitude of Δ tracked changes in the magnitude of χps, with a larger Δ from the cyclohexane solvent (with $\chi ps \sim 2.0$ kT) than from the carbon tetrachloride solvent (with $\chi ps \sim 1.0$ kT). Estimates of Δ for adsorption of a dimethylamino end group were made in the same way and amounted to ~12.4 kT from carbon tetrachloride onto Aerosil 130 silica and ~18.8 kT from cyclohexane onto Aerosil 130 silica. As expected, the values of Δ for adsorption of the dimethylamino end group were measured as substantially higher than measures of Δ for the carboxylic acid end group onto Aerosil 130 silica, for reasons outlined previously in the text. As expected also, Δ for adsorption of this end cap from cyclohexane exceeded substantially the magnitude of Δ for adsorption from carbon tetrachloride onto this substrate.

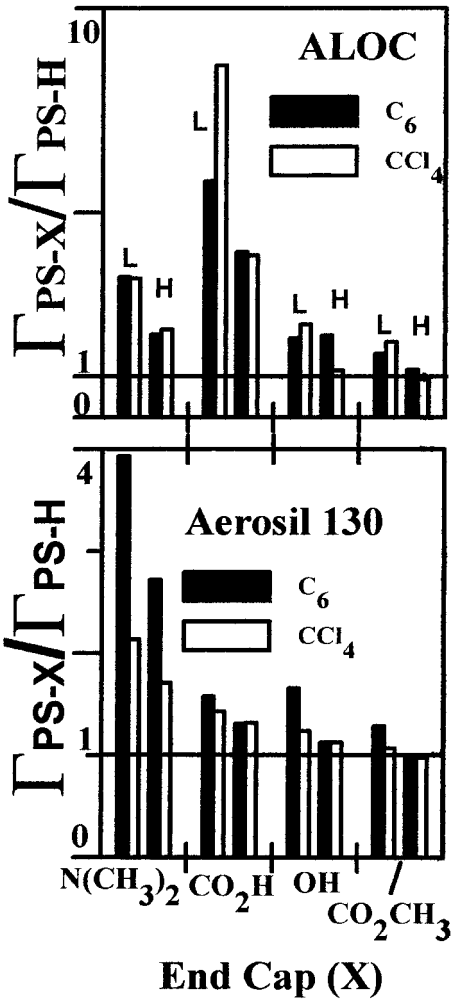

Figure 10 Bar charts showing the experimentally determined dimensionless ratio ΓPS–X/ΓPS–H for polymers of matched molecular weight, adsorbed from cyclohexane (C6) or from carbon tetrachloride (CCl_4) onto ALOC or onto Aerosil 130 silica. Lower molecular weight pairs of polymers (20 kD) are designated L, while higher molecular weight polymers (300 kD) are designated H on the chart.

In contrast, we do not have a reliable measure of χps for polystyrene adsorbing onto activated

strongly basic aluminum oxide C or ALOC (except that $0.1 \ll \chi ps < 1$ for adsorption from CCl_4 and $1 \ll \chi ps < 2$ for adsorption from cyclohexane). For this reason, we cannot estimate the values of Δ, for end groups on polymers adsorbing onto ALOC from plots of $\Gamma x/\Gamma_H$ versus Δ, constructed as above. To explore the concept of expressing Δ, as a multiple of χps for this substrate, we constructed plots of $\Gamma x/\Gamma_H$ versus $\Delta/\chi ps$, as illustrated in Figure 12, for adsorption of a polymer of degree $N = 200$ from a theta solvent (top) and from a good solvent (bottom). Unfortunately, the ratio $\Gamma x/\Gamma_H$ (or y) at fixed Δ is revealed as a strong function of the absolute value of χps used in the SCF calculation, with the result that each unique value of $\Delta/\chi ps$ (or x) may be linked to multiple values of the ratio $\Gamma x/\Gamma_H$, depending on the magnitude of χps entered into the calculation for $\Gamma x/\Gamma_H$. These results give additional affirmation to the intuitive conclusion that an enhanced adsorption at a fixed Δ for the end group is inversely related to the magnitude of χps for the in-chain polymer segments.

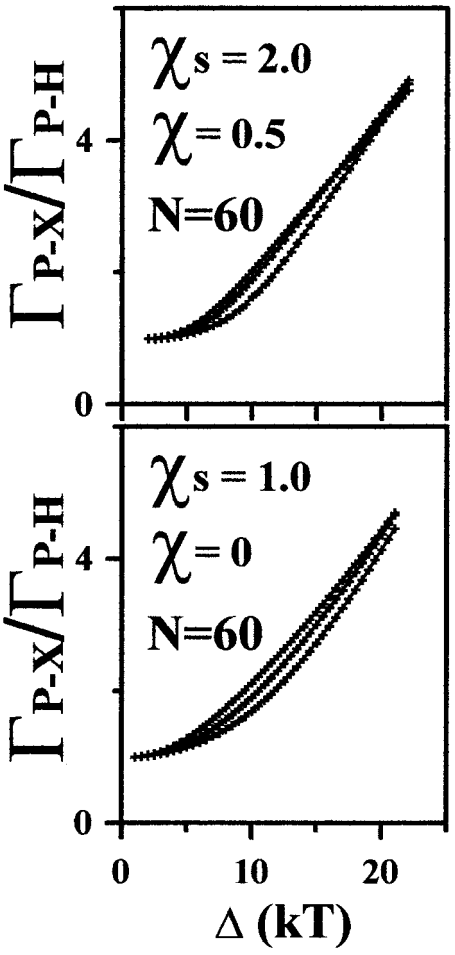

Figure 11 Plots of ΓP–X/ΓP–H versus Δ for $N = 60$ as calculated by SCF for three concentrations of polymer ($c = 0.1$, 1.0, and 5.0%) in solution. (Top) Adsorption from a theta solvent ($\chi = 0.5$) with χps set at 2.0 kT to simulate adsorption from cyclohexane onto silica. (Bottom) Adsorption from a good solvent ($\chi = 0$) with χps set at 1.0 kT to simulate adsorption from CCl_4 onto silica. (Data points have been omitted for clarity of presentation.)

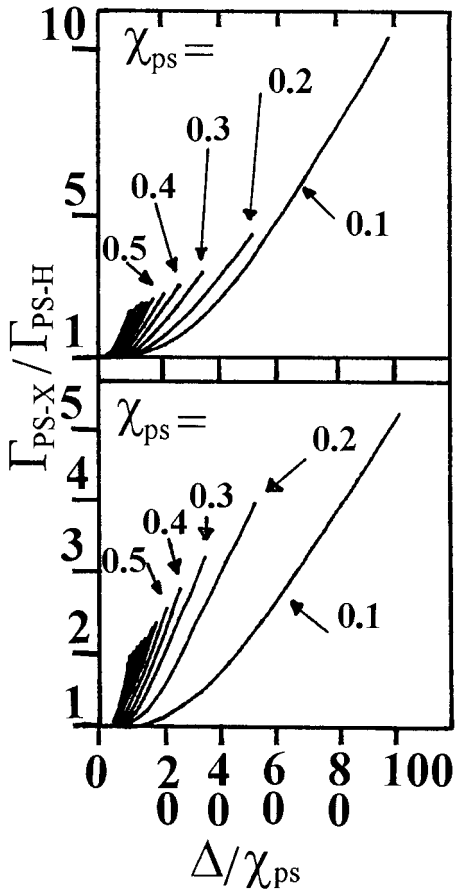

Figure 12 SCF calculations plotted to elucidate the dependence of the dimensionless ratio ΓPS–X/ΓPS–H, for a chain of length $N = 200$ as a function of the dimensionless ratio $\Delta/\chi ps$. (Top) Polymer adsorbed from a theta solvent ($\chi = 0.5$). (Bottom) Polymer adsorbed from a good solvent ($\chi = 0$). Individual curves are annotated with the value of χps used in the calculation of ΓPS–X/ΓPS–H (with 0.1 kT $< \chi ps <$ 1.0 kT in 0.1 kT increments).

The authors gratefully thank Dr. Kenneth Klabundy (Kansas State University) for the BET surface area measurements and Mr. Tom Denton (Oklahoma State University) for the construction of the specialty glass-

ware. This work was sponsored by the National Science Foundation under NSF-EPSCoR grant number OSR-9255223 with matching support from the State of Kansas.

REFERENCES

1. Ellerstein, S.; Ullman, R. J Polym Sci 1961, 55, 123.
2. deGennes, P. G. Adv Coll Interface Sci 1987, 27, 189.
3. deGennes, P. G. Scaling Concepts in Polymer Physics; Cornell University: Ithica, NY, 1979.
4. deGennes, P. G. Macromolecules 1980, 13, 1069.
5. Scheutjens, J. M. H. M.; Fleer, G. J. J Phys Chem 1970, 83, 1619.
6. Milner, S. T.; Witten, T. A.; Cates, M. E. Macromolecules 1988, 21, 1610.
7. Dijt, J. C.; Cohen Stuart, M. A.; Fleer, G. J. Macromolecules 1994, 27, 3219.
8. Dan, N. Macromolecules 1994, 27, 2310.
9. Kumacheva, E.; Klein, J.; Pincus, P.; Fetters, L. J. Colloids Surf A Physicochem Eng Asp 1994, 89, 283.
10. Kumacheva, E.; Klein, J.; Pincus, P.; Fetters, L. J. Macromolecules 1993, 26, 6477.
11. deGennes, P. G. In New Trends in Physics and Physical Chemistry of Polymers; Lee, L. H., Ed.; Plenum: New York, 1989.
12. Scheutjens, J. M. H. M.; Fleer, G. J. J Phys Chem 1980, 84, 178.
13. Semenov, A. N.; Joanny, J. F. Europhys Lett 1995, 29, 279.
14. vonGoeler, F.; Muthukumar, M. Macromolecules 1995, 28, 6608.
15. Singh, N.; Karim, A.; Bates, F. S.; Tirrell, M.; Furusawa, K. Macromolecules 1994, 27, 2586.
16. Li, H.; Witten, T. A. Macromolecules 1994, 27, 449.
17. Wijmans, C. M.; Zhulina, E. B. Macromolecules 1993, 26, 7214.
18. Zhulina, E. B.; Borisov, O. V. Macromolecules 1996, 29, 2618.
19. Shubin, V. Langmuir 1994, 10, 1093.
20. Linse, P. Macromolecules 1996, 29, 326.
21. Hoogeveen, N. G.; Hoogendam, C. W.; Tuinier, R.; Cohen Stuart, M. A. Int J Polym Anal Character 1995, 1, 315.
22. Kamiyama, Y.; Israelachvili, J. N. Macromolecules 1992, 25, 5081.
23. Davies, R. J.; Dix, L. R.; Toprakcioglu, C. J Colloid Interface Sci 1989, 129, 145.
24. Pefferkorn, E.; Jean-Chronenberg, A. C.; Varoqui, R. Macromolecules 1990, 23, 1735.
25. Auvray, L.; Cruz, M.; Auroy, P. J Phys II Fr 1992, 2, 1133.
26. Cohen Stuart, M. A.; Tamai, H. Macromolecules 1988, 21, 1863.
27. Cohen Stuart, M. A.; Fleer, G. J. Ann Rev Mater Sci 1996, 26, 463.
28. Taunton, H. J.; Toprakcioglu, C.; Fetters, L.;J.; Klein, J. Macromolecules 1990, 23, 571.
29. Klein, J.; Kamiyama, Y.; Yoshizawa, H;. Israelachvili, J. N.; Fredrickson, G.;H.; Pincus, P.; Fetters, L. J. Macromolecules 1993, 26, 5552.
30. Klein, J. Macromol Rep A 1992, 29(Suppl 2), 99.
31. Claesson, P. M.; Blomberg, E.; Froberg, J. C.; Nyler, T.; Arnebrant, T. Adv Colloid Interface Sci 1995, 57, 161.
32. Gallinet, J. P.; Gauthier-Manuel, B. Colloids Surf 1992, 68, 189.
33. Cosgrove, T.; Obey, T. M.; Ryan, K. Colloids Surf 1992, 65, 1.
34. Cosgrove, T.; Griffiths, P. C. Adv Colloid Interface Sci 1992, 42, 175.
35. Cosgrove, T. J Chem Soc Faraday Trans 1990, 86, 1323.
36. Leonhardt, D. C.; Johnson, H. E.; Granick, S. Macromolecules 1990, 23, 687.
37. Johnson, H. E.; Granick, S. Macromolecules 1990, 23, 3367.
38. Frantz. P.; Granick, S. Phys Rev Lett 1991, 66, 899.
39. Frantz, P.; Leonhardt, D. C.; Granick, S. Macromolecules 1991, 24, 1868.
40. Johnson, H. E.; Granick, S. Science 1992, 255, 966.
41. Johnson, H. E.; Douglas, J. F.; Granick, S. Phys Rev Lett 1993, 70, 3267.
42. Johnson, H. E.; Clarson, S. J.; Granick, S. Polymer 1993, 34,1960.
43. Frantz. P.; Granick, S. Macromolecules 1994, 27, 2553.
44. Schneider, H. M.; Granick, S.; Smith, S. Macromolecules 1994, 27, 4714.
45. Schneider, H. M.; Granick, S.; Smith, S. Macromolecules 1994, 27, 4721.
46. Lee, D. H.; Condrate, R. A.; Reed, J. S. J Mater Sci 1996, 31, 471.
47. Ren, Y.; Shoichet, M.S.; McCarthy, T. J.; Stidham, H. D.; Hsu, S. L. Macromolecules 1995, 28, 358.
48. Proteins at Interfaces; Brash, J. L.; Horbett, T. A., Eds.; ACS Symposium Series 343; American Chemical Society, Washington, DC, 1987; Chapters 21–23.
49. Pitt, W. G.;Cooper, S. L. Biomaterials 1986, 7, 340.
50. Kugo, K.; Okuno, M.; Kitayama, K.; Kitaura, T.; Nishino, J.; Ikuta, N.; Nishio, E.; Iwatsuki, M. Biopolymers 1992, 32, 197.
51. Jeon, J. S.; Sperline, R. P.; Raghavan, S. Appl Spectrosc 1992, 46, 1644.
52. Ishida, K. P.; Griffiths, P. R. Appl Spectrosc 1993, 47, 584.
53. Magnani, A.; Busi, E.; Barbucci, R. J Mater Sci Mater Med 1994, 5, 839.

54. Ong, J. L.; Chittur, K. K.; Lucas, L. C. J Biomed Mater Res 1994, 28, 1337.
55. Kim, M. W.; Fetters, L. J; Chen, W.; Shen, Y. R. Macromolecules 1991, 24, 4216.
56. Menius, C. F.; Ljunggren, L. Biomaterials 1991, 12, 369.
57. Malmsten, M. J Colloid Interface Sci 1994, 166, 333.
58. Pai-Paniker, R. S.; Dorgan, J. R.; Carlin, R. T.; Uyanik, N. Macromolecules 1995, 28, 3471.
59. Williams, D. R. M. Macromolecules 1993, 26, 5096.
60. Freij-Larsson, C.; Nyler, T.; Jannasch, P.; Wesslen, B. Biomaterials 1996, 17, 2199.
61. Cosgrove, T. Macromol Rep A 1992, 29(Suppl 2), 125.
62. Cosgrove, T.; Heath, T. G.; Ryan, K. Langmuir 1994, 10, 3500.
63. Auvray, L.; Auroy, P.; Cruz, M. J Phys I Fr 1992, 2, 943.
64. Bijsterbosch, H. D.; deHaan, V. O.; deGraaf, A. W.; Mellema, M.; Leermakers, F. A. M.; Cohen Stuart, M. A.; vanWell, A. A. Langmuir 1995, 11, 4467.
65. Perahia, D.; Wiesler, D. G.; Satija, S. K.; Fetters, L. J.; Sinha, S. K.; Milner, S. T. Phys Rev Lett 1994, 72, 100.
66. Auroy, P.; Auvrey, L. Macromol Rep A 1992, 29(Suppl 2), 117.
67. Lok, B. K.; Cheng, Y.-L.; Robertson, C. R. Colloid Interface Sci 1983, 91, 87.
68. Knoll, W. Makromol Chem 1991, 192, 2827.
69. Dijt, J. C.; Cohen Stuart, M. A.; Fleer, G. J. In Colloid–Polymer Interactions; Dubin, P. L.; Tong, P., Eds.; ACS Symposium Series 532; American Chemical Society, Washington, DC, 1993; Chapter 2.
70. Dijt, J. C.; Cohen Stuart, M. A.; Fleer, G. J. Macromolecules 1994, 27, 3207.
71. Couzis, A.; Gulari, E. Macromolecules 1994, 27, 3580.
72. Dorgan, J. R.; Stamm, M.; Toprakcioglu, C. Polymer 1993, 34, 1554.
73. Awan, M. A.; Dimonie, V. L.; Filippov, L. K.; El-Aasser, M. S. Langmuir 1997, 13, 130.
74. Amiel, C.; Sikka, M.; Schneider, J. W.; Tsao, Y.-H.; Tirrell, M.; Mays, J.W. Macromolecules 1995, 28, 3125.
75. Nygren, H.; Arwin, H.; Welin-Klintstrom, S. Colloids Surf A Physicochem Eng Asp 1993, 76, 87.
76. Clarke, C. J.; Jones, R. A. L.; Edwards, J. L.; Clough, A. S.; Penfold, J. Polymer 1994, 35, 4065.
77. Van de Ven, T. G. M. Adv Coll Interface Sci 1994, 48, 121.
78. Huguenard, C.; Pefferkorn, E. Macromolecules 1994, 27, 5271.
79. Cohen Stuart, M. A.; Cosgrove, T.; Vincent, B. Adv Colloid Interface Sci 1986, 24, 143.
80. Halperin, A.; Zhulina, E. B. Macromolecules 1991, 24, 5393.
81. Grest, G. S.; Murat, M. Macromolecules 1993, 26, 3108.
82. Zajac, R.; Chakrabarti, A. Phys Rev E 1994, 49, 3069.
83. Shull, K. R. Macromolecules 1996, 29, 2659.
84. Chen, H.; Chakrabarti, A. Phys Rev E 1995, 52, 3915.
85. Zajac, R.; Chakrabarti, A. Phys Rev E 1995, 52, 6536.
86. Zajac, R.; Chakrabarti, A. J Chem Phys 1996, 104, 2418.
87. Gilman, H.; Cartledge, F. K. J Organomet Chem 1964, 2, 277.
88. Eisenbach, C. D.; Schnecko, H.; Kern, W. Eur Polym J 1975, 11, 699.
89. Pispas, S.; Pitsikalis, M.; Hadjichristidis, N.; Dardini, P.; Mori, F. Polymer 1995, 36, 3005.
90. Mann, P. J.; Wen, S.; Xiaonan, Y.; Stevenson, W. T. K. Eur Polym J 1990, 26, 489.
91. Huggins, M. L. J Am Chem Soc 1942, 64, 2716.
92. Kraemer, E. O. Ind Eng Chem 1938, 30, 1200.
93. Vogel, A. E. Textbook of Practical Organic Chemistry, 4th ed.; Longman: New York, 1978; Chapter I-31.
94. Bhaskar, J. V.; Periasamy, M. J Org Chem 1991, 56, 5964.
95. Hashimoto, N.; Aoyama, T.; Shioiri, T. Chem Pharm Bull 1981, 29, 1475.
96. Technical Bulletin Pigments # 11; Basic Characteristics of Aerosil™; Degussa AG: Frankfurt am Main, Germany.
97. Technical Bulletin Pigments #56; Highly Dispersed Metal Oxides Produced by the Aerosil™ Process; Degussa AG: Frankfurt am Main, Germany.
98. Brunauer, S.; Emmett, P. H.; Teller, E. J Am Chem Soc 1938, 60, 309.
99. Scheutjens, J. M. H. M.; Fleer, G. J. J Phys Chem 1979, 83, 1619.
100. Kawaguchi, M.; Maeda, K.; Kato, T.; Takahashi, A. Macromolecules 1984, 17, 1666.
101. Cohen Stuart, M. A.; Fleer, G. J.; Scheutjens, J. M. H. M. J Colloid Interface Sci 1984, 97, 515.
102. Cohen Stuart, M. A.; Fleer, G. J.; Scheutjens, J. M. H. M. J Colloid Interface Sci 1984, 97, 526.
103. Kawaguchi, M.; Chikazawa, M.; Takahashi, A. Macromolecules 1989, 22, 2195.
104. Szwarc, M.; VanBeylen, M. Ionic Polymerization and Living Polymers; Chapman and Hall: New York, 1993.
105. Quirk, R. P.; Chen, W.-C. Makromol Chem 1982, 183, 2071.
106. Quirk, R. P.; Yin, J.; Fetters, L. J. Macromolecules 1989, 22, 85.

107. Ogle, C. A.; Strickler, F. H.; Gordon, B. Macromolecules 1993, 26, 5803.
108. Flory, P. J. J Am Chem Soc 1940, 62, 1561.
109. Szwarc, M. Carbanions, Living Polymers, and Electron Transfer Processes; Wiley-Interscience: New York, 1968.
110. Lyengar, D. R.; McCarthy, T. J. Polym Prepr 1989, 30, 154.
111. Slough, G. A. J Chem Ed 1995, 72, 1031.
112. Christophliemk, P.; Fahn, R.; Ferch, H.; Kreher, A.; Worms, K. H. Chemische Technologie B 3 Anorganische Technologie II, 4. Auflage S, 1983; p 57.
113. Peri, J. B. J. Phys Chem 1965, 69, 220.
114. Houwink, R. J Prakt Chem 1940, 157, 15.
115. Mark, H. Der feste Korper; Hirzel: Leipzig, 1938.
116. Danusso, F.; Moraglio, G. J Polym Sci 1957, 24, 161.
117. Grubisic, Z.; Rempp, P.; Benoit, H. Polym Lett 1967, 5, 753.
118. Howard, G. H.; Woods, S. J. J Polym Sci A-2 1972, 10, 1023.